Molecular Phylogenetics and Evolution

Incorporating mitogenome sequencing into integrative taxonomy: the multidisciplinary redescription of the ciliate Thuricola similis (Peritrichia, Vaginicolidae) provides new insights into the evolutionary relationships among Oligohymenophorea subclasses

--Manuscript Draft--

Manuscript Number:	
Article Type:	Research Paper
Keywords:	18S rRNA gene; Mitochondrial genome; Phylogenomics; Next Generation Taxonomy; Systematics; WWTP protists
Corresponding Author:	Giulio Petroni, Ph.D University of Pisa Pisa, ITALY
First Author:	Wanying Liao
Order of Authors:	Wanying Liao
	Pedro Henrique Campello-Nunes
	Leandro Gammuto
	Tiago Abreu Viana
	Roberto de Oliveira Marchesini
	Thiago da Silva Paiva
	Inácio Domingos da Silva-Neto
	Letizia Modeo
	Giulio Petroni, Ph.D
Abstract:	The evolutionary relationships among Oligohymenophorea subclasses are under debate as the phylogenomic analysis using a large dataset of nuclear coding genes is significantly different to the 18S rDNA phylogeny, and it is unfortunately not stable within and across different published studies. In addition to nuclear genes, the faster-evolving mitochondrial genes have also shown the ability to solve phylogenetic problems in many ciliated taxa. However, due to the paucity of mitochondrial data, the corresponding work is scarce, let along the phylogenomic analysis based on mitochondrial gene dataset. In this work, we presented the characterization on Thuricola similis Bock, 1963, a loricate peritrich (Oligohymenophorea), incorporating mitogenome sequencing into integrative taxonomy. As the first mitogenome for the subclass Peritrichia, it is linear, 38,802 bp long, and contains two rRNAs, 12 tRNAs, and 43 open reading frames (ORFs). As a peculiarity, it includes a central repeated region composed of tandemly repeated A-T rich units working as a bi-transcriptional start. Moreover, taking this opportunity, the phylogenomic analyses based on a set of mitochondrial genes were also performed, revealing that T. similis, as a representative of Peritrichia subclass, branches basally within the Oligohymenophorea class. Evolutionary relationships among Oligohymenophorea subclasses were discussed, also in the light of recent phylogenomic reconstructions based on a set of nuclear genes. Beside, as a little-known species, T. similis was also redescribed and neotypified based on data from two populations collected from wastewater treatment plants (WWTPs) in Brazil and Italy, by means of integrative methods (i.e., living observation, silver staining methods, scanning and transmission electron microscopy, and 18S rDNA phylogeny). After emended diagnosis, it is characterized by: (1) the sewage habitat; (2) the lorica with a single valve and small undulations; (3) the 7–22 μm-long inner stalk; and (4) the presence of only a single postciliary microtubule on the left side of the aciliferous row in the haplokinety. Among Vaginicolidae family, our 18S rRNA gene-based phylogenetic analysis revealed that Thuricola and Cothuriconia are monophyletic genera, and Vaginicola could be a paraphyletic genus.
Suggested Reviewers:	Alan Warren Natural History Museum

	a.warren@nhm.ac.uk Dr. Warren, whose research fields are systematics and biodiversity of ciliated protists. He is not only an excellent protistologist with many published articles, but also a board member of many international protist journals. Therefore, he can act as both a professional scholar and a valuable reviewer. Moreover, his doctoral research was on the ecology, morphology, and taxonomy of freshwater peritrich ciliates. Finally, he produced parts of the few ultrastructural investigations available so far on these ciliates.
	Gentekaki Eleni Mae Fah Luang University School of Science gentekaki.ele@mfu.ac.th Dr. Gentekaki's research topics are diverse, ranging from biodiversity of microbial eukaryotes to comparative genomics. Moreover, she is familiar with protist systematics, phylogenetics, molecular evolution and genomics as she had several publications on those topics. She undoubtedly can provide a professional review of the mitogenome and phylogenetics sections.
	Ping Sun Xiamen University psun@xmu.edu.cn Dr. Sun is a very professional scholar on the morphology and systematics of the subclass Peritrichia, Ciliophora. She produced a lot of valuable morphological works on peritrichs, with the establishment of new species, re-diagnosis of poorly known ones, etc. Meanwhile, she also contributed some works concerning molecular phylogeny of this group with phylogenetic reconstructions. Hence, she has a huge expertise on Peritrichia and can provide reliable opinions on our work.
Opposed Reviewers:	

November 14, 2020

Dear Editor,

We submit the enclosed manuscript entitled "Incorporating mitogenome sequencing into integrative taxonomy: the multidisciplinary redescription of the ciliate *Thuricola similis* (Peritrichia, Vaginicolidae) provides new insights into the evolutionary relationships among Oligohymenophorea subclasses" authored by Liao et al. to be kindly considered for publication in Molecular Phylogenetics and Evolution.

In this paper, we applied an integrative taxonomic approach to describe a little-known sewage peritrichous ciliate. We characterized two populations of *T. similis* from far related areas using morphological plus 18S rDNA sequence data. Moreover, we provided its ultrastructural description and the complete mitochondrial genome sequence (the first sequence for the subclass Peritrichia). Based on mitogenome sequencing, we could test evolutionary hypotheses within the class Oligohymenophorea. In contrast to the generally accepted 18S rDNA sequencing-based phylogeny, we observed that Peritrichia branches basally within the Oligohymenophorea class, as a sister taxon to all remaining subclasses. This result agrees with old morphology-based classification and with some recent phylogenomic data independently produced from nuclear coded gene. Finally, we discussed the importance of joining good morphological descriptions to molecular and genomic investigations, and suggested mitochondrial genome as a marker to be reevaluated for studies on ciliate systematics.

Considering the overall integration of data and their relevance in the studies of Oligohymenophorea, the most investigated class of Ciliophora, we think our paper could be of interest for publication in MPE.

The manuscript has not been previously submitted elsewhere, and all authors agreed to submit it to your journal.

All correspondence thereafter can be directed to Dr. Letizia Modeo (E-mail: letizia.modeo@unipi.it).

Thank you for considering our request!

Best regards,
Giulio Petroni

Highlights

- Redescription of a little-known ciliate by means of integrative taxonomy.
- First complete mitogenome for subclass Peritrichia (Oligohymenophorea).
- Phylogenomic analyses by using 20 concatenated mtDNA genes.
- Peritrichia branches as a sister group to Oligohymenophorea subclasses.

Graphical Abstract

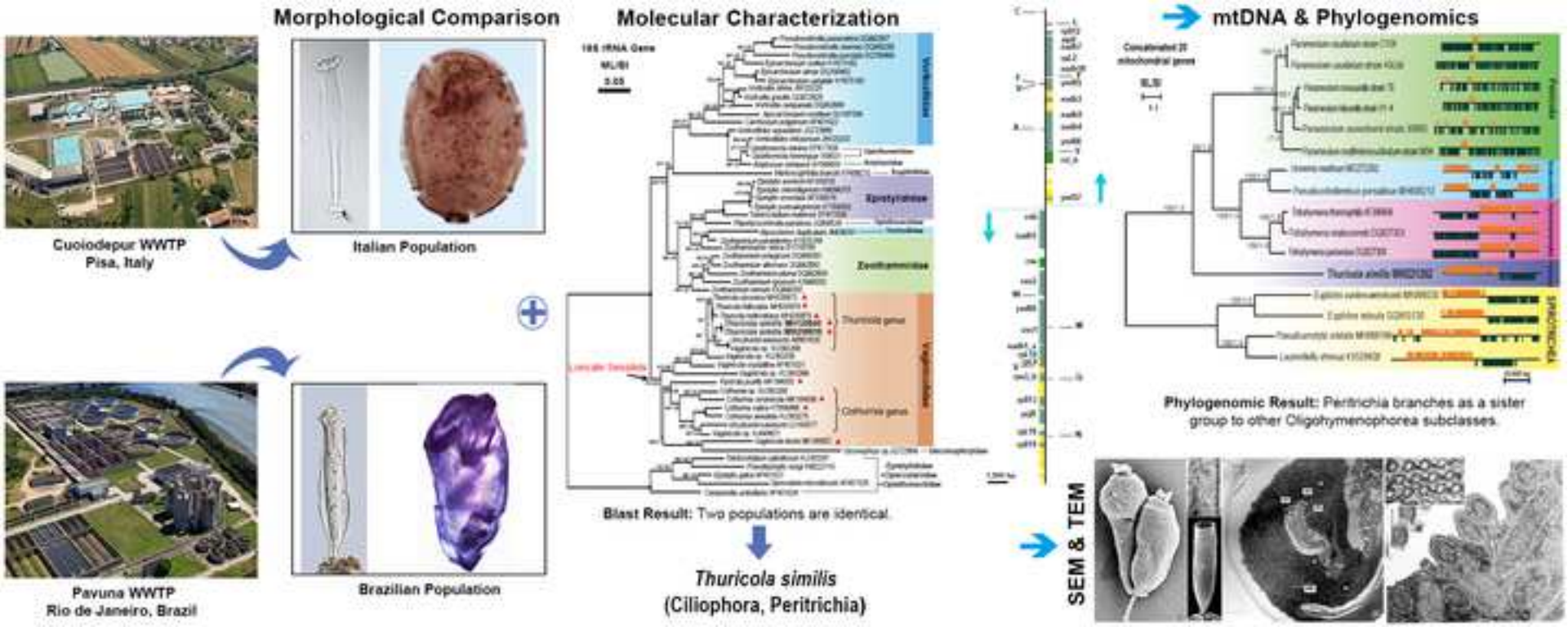

Incorporating mitogenome sequencing into integrative taxonomy: the multidisciplinary redescription of the ciliate *Thuricola similis* (Peritrichia, Vaginicolidae) provides new insights into the evolutionary relationships among Oligohymenophorea subclasses

Wanying Liao[1], Pedro Henrique Campello-Nunes[2], Leandro Gammuto[1], Tiago Abreu Viana[2], Roberto de Oliveira Marchesini[2], Thiago da Silva Paiva[2], Inácio Domingos da Silva-Neto[2], Letizia Modeo[1,3*], Giulio Petroni[1,3*]

[1]Department of Biology, University of Pisa, Via A. Volta 4/6, 56126, Pisa Italy

[2]Laboratório de Protistologia, Instituto de Biologia, Departamento de Zoologia, Universidade Federal do Rio de Janeiro, CEP: 21941-902 Ilha do Fundão, Rio de Janeiro, Brazil

[3]CISUP, Centro per l'Integrazione della Strumentazione Scientifica dell'Università di Pisa, Lungarno Pacinotti 43, 56126, Pisa, Italy

* Corresponding authors at: Department of Biology, University of Pisa, Via A. Volta 4/6, 56126, Pisa, Italy (G. Petroni, L. Modeo).
E-mail addresses: giulio.petroni@unipi.it (G. Petroni), letizia.modeo@unipi.it (L. Modeo).

ABSTRACT

The evolutionary relationships among Oligohymenophorea subclasses are under debate as the phylogenomic analysis using a large dataset of nuclear coding genes is significantly different to the 18S rDNA phylogeny, and it is unfortunately not stable within and across different published studies. In addition to nuclear genes, the faster-evolving mitochondrial genes have also shown the ability to solve phylogenetic problems in many ciliated taxa. However, due to the paucity of mitochondrial data, the corresponding work is scarce, let along the phylogenomic analysis based on mitochondrial gene dataset. In this work, we presented the characterization on *Thuricola similis* Bock, 1963, a loricate peritrich (Oligohymenophorea), incorporating mitogenome sequencing into integrative taxonomy. As the first mitogenome for the subclass Peritrichia, it is linear, 38,802 bp long, and contains two rRNAs, 12 tRNAs, and 43 open reading frames (ORFs). As a peculiarity, it includes a central repeated region composed of tandemly repeated A-T rich units working as a bi-transcriptional start. Moreover, taking this opportunity, the phylogenomic analyses based on a set of mitochondrial genes were also performed, revealing that *T. similis*, as a representative of Peritrichia subclass, branches basally within the Oligohymenophorea class. Evolutionary relationships among Oligohymenophorea subclasses were discussed, also in the light of recent phylogenomic reconstructions based on a set of nuclear genes. Beside, as a little-known species, *T. similis* was also redescribed and neotypified based on data from two populations collected from wastewater treatment plants (WWTPs) in Brazil and Italy, by means of integrative methods (i.e., living observation, silver staining methods, scanning and transmission electron microscopy, and 18S rDNA phylogeny). After emended diagnosis, it is characterized by: (1) the sewage habitat; (2) the lorica with a single valve and small undulations; (3) the 7–22 µm-long inner stalk; and (4) the presence of only a single postciliary microtubule on the left side of the aciliferous row in the haplokinety. Among Vaginicolidae family, our 18S rRNA gene-based phylogenetic analysis revealed that *Thuricola* and *Cothurnia* are monophyletic genera, and *Vaginicola* could be a paraphyletic genus.

Keywords: 18S rRNA gene, Mitochondrial genome, Phylogenomics, Next Generation Taxonomy, Systematics, WWTP protists

1. Introduction

The order Sessilida includes over 800 species of sessile peritrichs widely distributed in various aquatic habitats (Foissner et al., 1992; Foissner et al., 2010; Kahl, 1935; Lu et al., 2018; Lu et al., 2019; Lu et al., 2020; Lynn, 2008; Munir and Sun, 2018; Sun et al., 2009; Zhou et al., 2019; Zhuang et al., 2016). They are bacterivorous and microphagous, generally free-living but also as ecto- or endosymbionts (Clamp, 2005, 2006; Foissner et al., 1999; Irwin and Lynn, 2015; Lu et al., 2020; Lynn, 2008; Xu et al., 2011). Sessilids, as filter-feeding ciliates, are frequently abundant in wastewater treatment plants (WWTPs), playing a role in improving water quality and being used as a bioindicator for plant performance (Foissner, 2016; Madoni, 2011; Nicolau et al., 2001; Serrano et al., 2008). Unfortunately, there has been little progress on the systematics (i.e., modern techniques-based taxonomy and molecular phylogeny) of this large and ecologically valuable group, with many sessilid taxa lacking reports on their infraciliature and silverline system, as well as molecular data (Eperon, 1980; Foissner, 1981; Foissner et al., 1992; Foissner and Schiffmann, 1974, 1975; Lom, 1964; Warren and Paynter, 1991). Additionally, among the sessile peritrichs, loricate forms are largely neglected in comparison with aloricate ones (Li et al., 2008; Liang et al., 2019; Lu et al., 2018; Lu et al., 2019; Lu et al., 2020; Martin-Cereceda et al., 2007; Munir and Sun, 2018; Sun et al., 2017a; Sun et al., 2009; Utz et al., 2010; Wu et al., 2020; Zhou et al., 2019). The family Vaginicolidae is a species-rich group of loricate sessilids, with nearly 200 nominal species, although, among them, there are many synonyms and misidentifications (Corliss, 1979; Foissner et al., 1992; Kahl, 1935; Trueba, 1978, 1980; Warren and Paynter, 1991). Indeed, most of them show a nearly cylindrical lorica and a trumpet-shaped body when fully extended; meanwhile, some commonly used taxonomic features, such as zooids size, lorica size, and length of inner stalk, do not sufficiently diverge (or even overlap) among congeners or related genera (Foissner et al., 1992; Lu et al., 2018; Lu et al., 2019; Trueba, 1978, 1980; Warren and Paynter, 1991). Furthermore, as for *Thuricola* and *Vaginicola*, the presence or absence of valves in the lorica is the only feature previously recorded to distinguish them (Lynn and Small, 2002; Trueba, 1980). Assuming that the original descriptions of most species of these two genera are incomplete and their type species are not available (Biernacka, 1963; Bock, 1952, 1963; Hammann, 1952; Kahl, 1935; Kent, 1981; Küsters, 1974; Nusch, 1970; Sommer, 1951; Stiller, 1971), and considering that there are no redescriptions taking advantage from modern morphological techniques (Foissner, 1991), the identification of Vaginicolidae species is not trivial.

Despite the widespread use of the 18S rRNA gene in the study of ciliates systematics, sequence data remain scarce for vaginicolids. In the last two years, Lu et al. (2018) and Lu et al. (2019) have provided new contributions to this little-known group with detailed morphological studies and phylogenetic analyses. Nevertheless, many gaps in the understanding of the morphology, ultrastructure, and phylogenetic relationships of this group, still need to be filled.

In the past two decades, with the accumulation of ciliate 18S rRNA gene sequences and relevant phylogenetic studies, the limitations in taxonomic and phylogenetic studies based on this molecule have been disclosed (Chantangsi et al., 2007; Strüder-Kypke and Lynn, 2010; Zhao et al., 2013). Recently, mitochondrial genes (such as *cox1* and *cox2*) with higher evolutional rates have being increasingly used in ciliates taxonomy, both for phylogenetic analysis and for discriminating species with similar morphological features (Barth and Berendonk, 2011; Barth et al., 2006; Coyne et al., 2011; Gentekaki and Lynn, 2010; Kher et al., 2011; Park et al., 2019b). Unfortunately, compared with 18S rRNA gene, mitochondrial protein coding genes are difficult to obtain since most ciliate groups lack corresponding group-specific primers. Advancements in high-throughput

single-cell sequencing and bioinformatics have made possible the obtainment of complete mitochondrial genome which, in combination with integrative taxonomy, recently led to the proposal of a new study approach referred to as the "Next Generation Taxonomy" (Serra et al., 2020).

Although complete mitochondrial genomes have been used in phylogenomic studies to resolve ancient evolutionary events in other groups of organisms (Bae et al., 2004; Cameron et al., 2007; Cameron et al., 2012; Cameron et al., 2009; Dumilag et al., 2018; Fenn et al., 2008; Hassanin et al., 2005; Ilyasov et al., 2016), this approach has not yet been widely applied in ciliates whose available mitogenomes are rather scarce. Indeed, only few complete mitochondrial genomes of ciliates are available online (Barth and Berendonk, 2011; Brunk et al., 2003; Burger et al., 2000; Coyne et al., 2011; de Graaf et al., 2011; de Graaf et al., 2009; Gao et al., 2018; Li et al., 2018; Moradian et al., 2007; Park et al., 2019a; Serra et al., 2020; Swart et al., 2012), and none of them come from peritrichs. In the last few years, the evolutionary relationships among and within the classes of Ciliophora have been investigated through phylogenomic studies using transcriptomes (Feng et al., 2015; Gentekaki et al., 2014; Gentekaki et al., 2017; Grant et al., 2012; Jiang et al., 2019; Lasek-Nesselquist and Johnson, 2019; Lynn and Kolisko, 2017; Lynn et al., 2018; Pan et al., 2019; Sheng et al., 2018; Sun et al., 2017b; Wang et al., 2019). The availability of ciliates' mitogenomes would allow to compare these two approaches, i.e., phylogenomic using nuclear transcriptomes versus phylogenomic using mitogenomes, to test evolutionary relationship with two sets of genes that evolve rather independently.

Taken this on board, we herein present the results of combining mitogenome phylogenomic analysis with integrative taxonomy approach for studying the evolutionary relationships among Oligohymenophorea subclasses. The redescription and neotypification of the little-known sessile peritrich *Thuricola similis* Bock, 1963 were performed according to the criteria of the "Next Generation Taxonomy" (Serra et al., 2020). In detail, two populations of this ciliate were found in samples from Brazilian and Italian WWTPs and carefully identified by means of *in vivo* and silver staining investigations, as well as 18S rRNA gene sequence comparisons. The ultrastructural characterization and the complete mitochondrial genome of the species were carried out for the first time. A 18S rDNA gene-based phylogenetic analysis and a phylogenomic analysis based on mitochondrial genes were performed. The implications of our mitogenome phylogenomic analysis, suggesting an alternative reconstruction of the evolutionary relationships among Oligohymenophorea subclasses, are discussed in the light of the generally accepted view.

2. Material and methods

2.1. Sampling, cultivation, and morphological studies

Brazilian population of *Thuricola similis* was collected in the aeration tank of Pavuna WWTP in Rio de Janeiro, Brazil (22º48'7.668"S, 43º18'26.003"W), in 2016 and 2017. The water salinity was 0.41‰. Samples were brought to the laboratory, where polyspecific cultures were established in Petri dishes with fresh water and macerated rice grains to sustain growth of bacteria as food (Foissner, 1992a) and kept at room temperature. Italian population of *T. similis* was firstly collected on 19 March, 2016 from the aeration tank of Cuoiodepur WWTP in San Romano (Pisa, Italy) (43°41'44.5"N, 10°46'02.7"E) where the water temperature was 22.8 °C, pH 6.97, and salinity was 0‰. However, it is worth mentioning that we found *T. similis* (verified by means of 18S rRNA gene sequencing) many times at the same site during the investigation on ciliate community at Cuoiodepur between 2018 and 2019, in samples with salinity ranging from 5 ‰ to 10‰ (on average

10‰). Samples were brought to laboratory, where polyspecific cultures were established in Petri dishes and maintained by feeding them once a week with *Raoultella planticola* (Gammaproteobacteria) in CerophyllTM medium (Boscaro et al., 2012). All Italian samples and cultures were kept in incubator at a temperature of 19 ± 1 °C.

Concerning morphological studies, cells of both populations (i.e., Brazilian and Italian) were selected under stereoscopic microscope, and live specimens were studied in detail under a light microscope with Differential Interference Contrast (DIC) optics with magnification of 100–1,000×. The specimens were fixed with Bouin's fluid, then washed with distilled water, and stained with protargol following the protocols by Dieckmann (1995) and Wilbert (1975) modified by Foissner (1992b). The protargol powders used to stain Brazilian and Italian populations were "Proteinate d'Argent" (Roques, Paris, France) and manually synthesized powder produced following the method described by Pan et al. (2013), respectively.

For both populations, optical microscopy pictures were captured with digital camera and used to obtain dimensions of living and stained ciliates. Morphometric measurements of the Italian and Brazilian populations were analyzed with ImageJ 1.46r software (Ferreira and Rasband, 2012) and Axion Vision SE64 software, respectively.

Drawings were obtained from living individuals and protargol stained specimens for both populations. They were handmade with the help of a camera lucida and nankin ink and edited with Adobe Photoshop CS6. Terminology used is mainly according to Trueba (1980) and Lynn (2008).

Scanning Electron Microscope (SEM) observation was performed on both populations, whereas Transmission Electron Microscope (TEM) observation was performed only on individuals from the Brazilian population of *T. similis*. SEM preparations and observations of the Brazilian population were according to da Silva-Neto et al. (2012) with a JEOL JSM-6510 SEM; Italian population was processed for SEM according to Nitla et al. (2019) and observed with a JEOL JSM-5410 SEM. TEM preparations were obtained according to da Silva-Neto et al. (2012) and observed under a MORGANI 228 TEM.

2.2. DNA isolation, amplification, and sequencing

Genomic DNA of 20 cells of the Brazilian population was extracted using DNeasy® Blood & Tissue Kit in accordance with manufacturer's protocols. The 18S rRNA gene was amplified using the universal eukaryotic primers: Euk A (5´-AACCTGGTTGATCCTGCCAGT-3´) and Euk B (5´-TGATCCTTCTGCAGGTTCACCTAC-3´) (Medlin et al., 1988). DNA amplification was done with PCR master mix polymerase of Promega according to the following thermal profile: one cycle by two minutes at 94°C followed by 35 cycles consisting of 30 seconds at 94°C, 30 seconds at 50 °C, and concluding with a final extension of two minutes at 72 °C. The PCR products were purified using the QIAquick PCR Purification Kit (Qiagen) following the manufacturer's protocols, and directly sequenced in the Laboratório de Protozoologia, Universidade Federal de Juiz de Fora, using the same set of primers used for amplification. Sequences were visualized using Geneious program and manually edited and assembled. The almost full-length of the 18S rRNA gene of the Italian population was obtained following the procedures described by Nitla et al. (2019) starting from 10–15 cells.

2.3. Whole genome amplification and assembly

Four cells of the Italian population were isolated from laboratory cultures, and then washed three times with distilled water. Total DNA material was amplified via whole genome amplification

(WGA) method, using REPLI-g Single Cell Kit (QIAGEN®, Hilden, Germany), following the manufacturer's instructions. The so obtained DNA material was processed with a Nextera XT library and sequenced at Admera Health (South Plainfield, USA), using Illumina HiSeq X technology to generate 14,536,622 reads (paired-ends 2×150 bp). Preliminary assembly of resulting reads was performed using SPAdes software version 3.6.0 (Bankevich et al., 2012).

2.4. Mitochondrial genome assembly and annotation

Starting from the preliminary assembly, contigs representing the mitochondrial genome of *Thuricola similis* were identified via BLAST analyses using other oligohymenophorean mitochondrial genomes as references. According to the BLAST result, we selected all the contigs with a GC content comprised between 18% and 25%, and with a coverage between 100× and 250×. Reads mapping on those contigs were selected from the raw data and reassembled using SPAdes software. The so assembled mitochondrial genome was annotated with PROKKA version 1.10 (Seemann, 2014) using the DNA translation codon table "4", and then manually inspected.

2.5. Phylogenetic and phylogenomic analyses

The two obtained 18S rRNA gene sequences of *Thuricola similis* were assembled using Chromas Lite version 2.1 software and compared with the non-redundant sequence database using BLAST, then aligned using the editor and alignment tools from the ARB software package version 5.5 (Westram et al., 2011) together with related sequences contained in the SSU refNR99 SILVA database (Quast et al., 2012) and some latest released sequences on GenBank database. In order to construct a more robust phylogeny of the family Vaginicolidae and reveal the systematic position of *Thuricola* genus within it, all available Vaginicolidae sequences longer than 1,400 bp were used, including two high quality environmental sequences that cluster within the investigated group (i.e., uncultured eukaryote AB901620 and LC150077). A total of 55 sequences of representative sessile peritrichs were employed in phylogenetic analyses: 19 were loricate representatives, including our two newly obtained sequences, and the remaining 36 were aloricate ones. *Campanella umbellaria*, *Epistylis galea*, *Opercularia microdiscum*, *Pseudepistylis songi*, and *Telotrochidium cylindricum* were selected as outgroup taxa. After manual editing to optimize base pairing in the predicted rRNA stem regions in this dataset, the alignment was reduced in length based on the shortest sequence, producing a 1,723-character matrix. Maximum likelihood (ML) tree was calculated with the PHYML software version 2.4 (Guindon and Gascuel, 2003) from the ARB package, using the GTR + I + G substitution model according to the program jModelTest 2 (Darriba et al., 2012). The nodal support was assessed by performing 1,000 pseudo-replicates. Bayesian inference (BI) analysis was performed with MrBayes version 3.2 (Ronquist et al., 2012) using the same substitution model as ML analysis. Three different Markov chain Monte Carlo (MCMC) runs were used, with one cold chain and three heated chains, with a burn-in of 25%, iterating for 1,000,000 generations.

For the phylogenetic analysis of *T. similis* using the whole mitochondrial genome, 11 species with complete mitochondrial genomes in the class Oligohymenophorea were selected as ingroup, and four species in the class Spirotrichea were selected as outgroup taxa. Among them, six *Paramecium* mitochondrial genomes (namely *P. biaurelia* strain V1-4, *P. caudatum* strain C104, strain 43c3d, *P. multimicronucleatum* strain M04, *P. novaurelia* strain TE, and *P. sonneborni* strain 30995) were downloaded from ParameciumDB (https://paramecium.i2bc.paris-saclay.fr) (Arnaiz et al., 2020), while the rest were taken from GenBank with their accession numbers shown in Fig. 10. Specifically, 20 protein coding genes with at least 90% presence in the mitochondrial genomes

of the above-mentioned species were selected for analysis. In Supplementary Table S2, you can find the list of analyzed 20 genes and their presences in all 16 species. The relative amino acidic sequences predicted from each protein coding gene were aligned using MAFFT software version 7.471 (Katoh and Standley, 2013). Then, we concatenated the multi-alignments of all 20 genes (gaps were inserted in few rare cases where a protein was missing from a certain species), and finally obtained an employed matrix composed by 10,248 sites. The best substitution model was estimated with ProtTest version 3.2 (Darriba et al., 2011), while RaxML software version 8 (Stamatakis, 2014) was used to estimate ML phylogeny with 100 bootstraps. BI analysis was performed with MrBayes version 3.2 using the best available model, Vt + F + G. Three different MCMC runs were used, with one cold chain and three heated chains, with a burn-in of 25%, iterating for 1,000,000 generations. A topology test was performed to assess whether alternative hypotheses were significantly different from our retrieved phylogenomic tree would be supported. Different trees were obtained arbitrarily collocating *T. similis* in different positions related to the various retrieved clades. Tests were performed on the IQ-TREE software version 1.6.12 (Nguyen et al., 2015) using RELL method (Kishino et al., 1990) with 10,000 replicates.

3. Results

3.1. General morphology based on Brazilian and Italian populations

The morphological data of the two studied populations were generally in accordance with each other, as visible in Table 1. Therefore, the redescription of *Thuricola similis* herein presented is based on data from both populations.

Colourless zooids solitarily living or sharing a lorica in groups of maximum three, anisometric individuals (Figs. 1A–E, 2A–G,K,M). Relaxed cells slender trumpet-shaped with anterior region enlarged and posterior region tapering towards the stalk, 136–314 × 9–19 µm *in vivo* (Table 1 and Figs. 1A–D, 2A,B,D,E–G,J), and contracted forms cylindrical, 53–112 × 17–38 µm *in vivo* (n=16) (Figs. 1E, 2C,K,M). Zooid very flexible: when fully extended, usually projecting nearly 1/4 to 1/3 of its body beyond aperture of lorica and slightly bending; when disturbed, shrinking back into lorica with ellipsoid or broadly conical in outline (Figs. 1A–E, 2A–G,K,M).

Single-layered peristomial collar, relatively thin (about 6 µm) and conspicuously everted, about 21–41 µm in diameter (Table 1 and Figs. 1A–D, 2A,B,D,F–H,J). Peristomial disc, about 21 µm in width, moderately elevated, and oblique in relation to the peristomial collar, with the plane and smooth surface (Table 1 and Figs. 1A–D, 2A,B,D,F–H,J). Oral infundibulum, about 38 µm in length, obliquely extending towards cell center (Table 1 and Figs. 1B–D, 2F,J). Trochal band forming a circular bulge near the mid-region of zooid *in vivo* (Figs. 1A,B,D, 2A,B,E,I,J). Pellicular ridges inconspicuous at low magnifications but distinct above 400 × magnification, about 136–232 transverse striations in total (Table 1 and Figs. 1A–D, 2I,N). In detail, 83–117 striations roughly counted from peristome to trochal band and 80–94 from trochal band to scopula *in vivo* for the Italian population (Table 1). This pellicular architecture was also verified in SEM processed aloricate contracted zooids, with (average) 0.16 µm thick annular striations encircling the body (Figs. 4C–E). In detail, the first 15–20 striations, beginning from the peristomial border, usually convoluted and slightly oblique to the front left, loosely aligned with each other (Fig. 4D), while the rest displayed a much more ordered arrangement, i.e., they nearly run straight, being spaced apart about 0.05–0.08 µm, and parallel to one another (Figs. 4C, E). Trochal band shown as four specialized rows of closely spaced striations which encircles the zooids according to SEM observation (Fig. 4E), about 0.7 µm wide. Zooids sharing the same stalk, 7–22 × 2–4 µm in size,

attached to the base of lorica with sometimes both ends slightly widened (Table1 and Figs. 1A–E, 2A–C,J,K,M,N, 4C).

A single contractile vacuole located at the level of peristomial collar near the dorsal wall of vestibulum (Figs. 1B,D,E, 2H,J). When completely full, contractile vacuole occupying almost all peristomial region, about 16 μm across (Table 1). Cytoplasm highly granulated. Food vacuoles of different sizes (3–13 μm) with bacteria and flagellates inside, usually scattered in the anterior third region of the cell, those at cell front showing a larger size (Table 1 and Figs. 1A–E, 2A–G,J,K,M). Cytoproct not observed. Macronucleus twisted band-shaped longitudinally oriented in zooid, with anterior region broader than the posterior; micronucleus slightly ellipsoid, near to posterior macronuclear end (Figs. 1G, 3H,I).

Lorica about 139–210 μm long, transparent and colourless, roughly cylinder-shaped, erect, attached directly to the substratum without a stalk (Table 1 and Figs. 1A–F, 2A–F,K–M). Aperture of lorica elliptical, posterior third to fourth of lorica gradually tapered towards the end, with base sometimes expanded (Figs. 1A–F, 2A–F,K–N). When view from the wide side, lorica nearly symmetrical with width at aperture 39 μm, midpoint 44 μm, base 16 μm; while from narrow side, asymmetrical, widest part being near the middle or posterior third, and anterior third being neck-like (Table 1 and Figs. 1A–F, 2A–F,K–M). One valve located nearly in the upper third to fourth of lorica, 31–46 μm long, some individuals with an additional, inconspicuous spine on the valve (Table 1 and Figs. 1B,E,F, 2C,F,G,K,L). A conspicuous bulge could be frequently found no far above the valve, when viewed from narrow side (Figs. 1B,F, 2C,K,L). Inside the lorica, a junctional membrane (i.e., funnel-shaped membrane according to Lu et al. (2018)) present to protect the contracted cell (or cells), probably beginning at the stalk and ending with the connection of valve (Figs. 1B,D, 2A,C,E,F,N). SEM observation revealed no lips in the lorica aperture and confirmed DIC observation that its surface is smooth at high magnification with some rod-shaped or filamentous bacteria attached (Figs. 4A,B). Irregular small undulations in lorica wall present in some individuals (Figs. 1D, 2C,E,M).

Peristomial ciliature surrounding the disc-shaped peristomial area composed of haplokinety and polykinety, with approximately 15 μm-long cilia (Figs. 1A–C,H, 2A,F,H,J, 3B,C). Polykinety and haplokinety composed of three and two rows of kinetosomes, respectively (Figs. 3C,E). They commence to run around peristome at almost the same position, parallel to each other, and separate at the entrance of infundibulum after approximately 1.5 turns (Figs. 1H, 3A–C). Within infundibulum, haplo- and polykinety making a further circuit on opposite walls and terminating near cytostome. Then, polykinety transforming into three infundibular polykineties (P1–P3), each consisting of three rows of kinetosomes (Figs. 1H, 3A,F,G). In detail, P1 and P2 nearly equal in length, and both longer than P3 (Figs. 1H, 3A,F,G). P2 interposed between P1 and P3 at the adstomal end (Figs. 1H, 3A,F,G). Row 1 of P2 merging with P1 abstomally and row 3 divergent from other two rows abstomally (Figs. 1H, 3A,F,G). P3 converging with P1 at the adstomal end (Figs. 1H, 3A,F,G). Row 1 of P3 extremely long, about twice to three times as long as two other rows (Figs. 1H, 3A,F). Since the outer two rows of P3 are equal in length and very proximal to each other, they sometimes overlapped in stained specimens (Fig. 3F). Epistomial membrane 1 located near the entrance of infundibulum; epistomial membrane 2 located ahead of the distal end of haplokinety and polykinety (Figs. 1H, 3B). Germinal kinety accompanying the infundibular part of haplokinety (Figs. 1H, 3A,E). After protargol staining, about 60–110 heavy stained kinetosomes visible at trochal band, setting closely in rows and encircling the body (Figs. 1H, 3D,H). Only at the mobile telotroch stage those basal bodies can develop the cilia, known as aboral ciliary girdle. Some basal bodies also shown in the scopula of an aloricate zooid specimen (Fig. 3D).

3.2. TEM observation

3.2.1. Lorica

Lorica 0.5 µm thick, with smooth internal and external surfaces (Figs. 5A,B, 6B,C). Lorica consisting of amorphous microfibrillary material, probably of protein origin (Figs. 6B,C).

3.2.2. Pellicle

Pellicle composed of an external plasma membrane, an inconspicuous alveolar layer, and a very electron-dense epiplasm (Fig. 6A). Underlying the pellicle, there are a slightly electron-dense myonemal layer (Fig. 6B) that is thicker in the upper two thirds of the zooid and thinner in the basal third. Myonemal layer particularly well developed and conspicuous in the peristomial collar region, forming a kind of thick ring, working as a sphincter to promote the closure of peristome (Fig. 6B). Pellicle also showing numerous small ridges perpendicular to the oral-aboral axis (Figs. 5C, 6A).

3.2.3. Oral ciliature

Peristomial ciliature consisting of a haplokinety and a polykinety (Figs. 5A,C). Haplokinety located in upper position in comparison with the polykinety, and composed of pairs of kinetosomes, of which only the outer row bears cilia (Figs. 5D, 6F). Polykinety composed of three rows of ciliferous kinetosomes (Figs. 5A,C,D). A thin ectoplasmic ridge separating haplokinety from polykinety (Fig. 5C). At the entrance to infundibulum, haplokinety and polykinety diverging, and polykinety transforming into three infundibular polykineties, P1–P3, each consisting of three rows of kinetosomes. P1 and P2 appearing next to the adstomal end of the P3, running in parallel with each other (Fig. 5B).

In the haplokinety, kinetosomes of the aciliferous row with only one postciliary microtubule on the left side (Fig. 6F). Associated to each kinetosome of the left row of the polykinety, a fibrillar band (*lame dense* according to Eperon and Grain (1983)) positioned towards the cell posterior part (Fig. 6G); the connection between anterior and posterior kinetosomes in the same row of the polykinety, consisting of two microtubules surrounded by a dense material (Figs. 6G,H). Basal microtubules running perpendicularly to the polykinety base (Fig. 6H). Infundibulum ending at the cytostome, next to the oral ribs, which resembles microvilli (Figs. 5A, 6D,E), i.e., arranged in a compact serrated form, with two microtubules on the left and four on the right side, playing a structural role (Figs. 5A, 6D,E).

3.2.4. Endoplasm

Endoplasm filled with opaque electron-dense granules, food vacuoles, mitochondria, and numerous endosymbiotic bacteria (Figs. 7A–D). Mitochondria showing inconspicuous lamellae (Fig. 7C). Endosymbiotic bacteria especially occurring at the epistomial disc and around the infundibulum (Figs. 7A,B). Endosymbiotic bacteria in binary fission also observed (Fig. 7D), as well as bacteria surrounded by many mitochondria, diffusely throughout the endoplasm (Figs. 7A–D).

3.2.5. Nucleus

Macronucleus containing heterochromatin (Fig. 5B), running along the longitudinal cell axis, occupying almost entire cell length, and making a significant transverse turn in the upper third of the cell. Micronucleus not observed.

3.3. Notes on autecology

Loricae of *Thuricola similis* were attached to activated sludge flocs, organic matter, and debris (Figs. 1A,C,D, 2A–E, 4A). Additionally, for the first time, they were seen attached to conspecifics' loricae as well (Figs. 2C,K, 4B). Besides, we found *T. similis*'s loricae attached to those of the ciliate *Chaetospira muelleri* Lachmann, 1856, and to the empty loricae of *Arcella* sp., a testate amoeba. Based on these observations, apparently *T. similis* chose its substrate randomly, since it was observed attached to both unanimated and living substrate. In a rare condition, three zooids were observed inside the same lorica, sharing the same stalk (Figs. 2C,D). *T. similis* could be gregarious, since we observed pseudo-colonies with up to five loricae occupying the same substrate. A microconjugant, trophont-form, which had recently left its stalk and lorica, about 45 μm long, was also observed (Fig. 2G). Since *Thuricola* spp. are not extremely "homelovers", empty loricae were found (Figs. 1F, 2K,L), along with some trophont zooids, swimming freely in water using the peristomial cilia (Fig. 2J). Neither dividing organisms nor telotrochs were observed. *T. similis* is usually found in freshwater sewage, although it has also been proved to be stably present when salinity reaches 10‰, showing the adaptability to salinity variations. Due to sewage habitat, over the lorica surface, some (filamentous and/or rod) bacteria, organic matters, or debris (Figs. 1D, 2A,E,F,K, 4A,B) were observed. After a long period of colonization, those attached matters continued to accumulating on the surface of loricae, and occasionally invaded the inside of empty loricae (Fig. 2K).

3.4. Mitochondrial genome

The complete mitochondrial genome of *Thuricola similis* resulted in a singular linear contig of 38,802 bp, with a GC content of 22.7‰. It was deposited in GenBank database with the accession number MW221262. Its gene content was composed by 43 open reading frames (ORFs), 12 tRNA genes, a partial 16S rRNA gene (*rnl*-b), and a 12S rRNA gene (*rns*) (Fig. 8). In 20 out of the 43 predicted ORFs, protein coding genes (Supplementary Table S2) that were clearly homologous to genes of defined function (such as genes encoding components of the electron transport chain and ribosomal protein genes) in other mitochondrial genomes, were found. Four ORFs, namely *ymf*57, 65, 66, and 68, were genes without an identified function, but they had evident homologs in mitochondrial genomes of other oligohymenophoreans (like *Paramecium*, *Tetrahymena*, *Uronema*, and *Pseudocohnilembus*); besides, *ymf*65 was also found in *Oxytricha trifallax*. All those four genes were annotated and possibly considered "ciliate-specific" ORFs. The rest 19 ORFs appeared to be unique to *T. similis* with no detectable sequence similarity to known genes via automatic prediction or using BLASTP analysis against other ciliates mitochondrial genomes. Besides, there was a pure A-T repeat region in the middle of the mitochondrial genome of *T. similis*, making up of 19 base pairs tandemly repeated five times (Fig. 8), and working as a bi-directional transcription start.

3.5. Phylogenetic and phylogenomic analyses

The almost full length and partial 18S rRNA gene sequences of *Thuricola similis* were obtained from the Italian and Brazilian populations, and deposited in GenBank with accession number MW208818 (length: 1692bp, excluding PCR primers, 41.9% GC) and MH120840 (length: 1473bp, excluding PCR primers, 41.2% GC), respectively. The sequences of these two populations were identical to each other (in detail, the first (1^{st}) and last (1473^{th}) nucleotides of Brazilian population's sequence corresponded to the 68^{th} and 1540^{th} of Italian population's one, respectively). The most similar species were *T. folliculata* (Chinese population, MH035974) and *T. obconica* (Chinese

population, MH035973), both differing from *T. similis* at 12 different nucleotides sites in the dataset. *T. kellicottiana* (Chinese population, MH035975) differed from *T. similis* at 17 substitutions.

Both phylogenetic trees generated with ML and BI methods were congruent with respect to major nodes, so for the purpose of illustration, only the ML tree was shown in Fig. 9, with nodal support provided for both algorithms. In the phylogenetic tree, all loricate sessilids represented a distinct branch from the aloricate ones, although with a relatively low support (61% ML, 0.93 BI), and were composed of two major clades. The first clade included all *Thuricola* and some *Vaginicola* species. In detail, the two populations of *T. similis* (MW208818 and MH120840) clustered together in a fully supported (100% ML, 1.00 BI) clade (as they were identical), which in turn grouped together with a *Vaginicola* sp. (KU363269) and the sequence of an uncultured ciliate (AB901620). These clustered together with *T. folliculata* (MH035974) and *T. kellicottiana* (MH035975) in the ML tree with low (38%) support, whereas formed a polytomy in the BI. As for the rest of *Thuricola* sequences available in GenBank, *T. obconica* (MH035973), was recovered as a sister taxon to the above mentioned *Thuricola-Vaginicola* assembly in both ML and BI analyses (67% ML, 0.96 BI), and then this group gathered with three vaginicolas (KU363258, AF401521, and KU363266) forming one major branch with low support value (51% ML, 0.90 BI). The second major clade was also relatively low supported (66% ML, 0.71 BI) and comprised four species of *Cothurnia* (KU363268, MK184556, KT956998, and KU363275), two species of *Vaginicola* (KJ649621, MK184557), *Pyxicola pusilla* (MK184555), an uncultured ciliate (LC150077), and *Usconophrys* sp. (JQ723986).

The phylogenomic tree based on 20 concatenated mitochondrial protein coding genes using two algorithms (ML and BI analysis) were consistent, therefore only the topology of ML was presented with support values from both algorithms indicated on branches (Fig. 10). In the tree, *T. similis* grouped with other oligohymenophorean ciliates and early branched from them, with a high statistical support. However, alternative tree topology test did not completely reject the possibility that *T. similis* forms a sister clade to the subclass Peniculia (Fig. 11H1) or branches within the clade composed of Hymenostomatia and Scuticociliatia subclasses (Fig. 11H3), while it completely denied the possibility of *T. similis* as a sister taxon to the subclass Hymenostomatia (Fig. 11H2). According to the statistical support of all verified hypotheses, Hypothesis 4 in Fig.11, the same as our retrieved topological structure, was undoubtedly the most robust one, where *T. similis* was the earliest branch within the Oligohymenophorea class.

4. DISCUSSION

4.1. Morphological comparison among populations of *Thuricola similis* and similar congeners

Thuricola similis was originally found in activated sludge of the Marl Chemical Park, located in North Rhine-Westphalia (Germany) by Bock (1963), who performed living observation on its lorica and zooids characters. Subsequently, Trueba (1980) revised the genus *Thuricola* and mentioned this species again based on Bock's population, providing the following diagnosis: lorica 158–248 μm long (mean 183 μm), cylindrical in shape, but tapering slightly towards the base; aperture 45 μm in diameter; stalk 10–20 μm long; lorica wall not smooth, but somewhat irregular, with undulations. Since then, only a brief morphological description on an Ukrainian population found in the activated sludge tank of a sewage treatment plant from Zhytomyr has been reported (Konstantynenko, 2007). Recently, Shen and Gu (2016) reported a freshwater form under the name of *T. similis* collected from Donghu Lake, Wuhan, but its rather bigger (300–500 μm long) zooids, shorter (7–9 μm) stalk, and lake habitat are instead reminiscent of *T. folliculata* (Foissner et al.,

1992). Thus, this should be considered a misidentification. All previous publications on *T. similis* are very brief and mainly based on living observation, the ciliature and molecular characterizations of this species have never been revealed, therefore a redescription following modern, integrated taxonomical criteria seems necessary for the sake of clarification.

Our two studied populations of *T. similis* from Brazil and Italy are basically in agreement with each other and correspond well to the type population (Bock, 1963) and previous descriptions (Konstantynenko, 2007) with respect to the basic morphological characters (e.g., zooids and lorica size, lorica structure, valve number, inner stalk length) and habitat (sewage water) (Tables 1, 2). A difference between Brazilian and Italian populations is the length of zooid (longer in the former, while shorter in the latter) (Tables 1, 2). It is logical to associate the size of zooids with the number of zooids sharing the lorica. Hence, the difference in zooid length of these two populations also reflects the difference in the number of zooids found in a single lorica: Brazilian population was observed to have up to three zooids sharing the lorica, while the maximum zooids present in the Italian population were two. Besides, some individuals of the Italian population exhibited a spine in the valve, although inconspicuous. This minor morphological difference was not mentioned in previous works, and we think it may have been overlooked. However, since this spine was not found in all observed Italian individuals, we did not consider it as a sufficiently stable morphological character for population discrimination. Finally, Italian population of *T. similis* has been repeatedly found in a habitat where the salinity can reach 10‰, while other populations have mostly been recorded in freshwater sewage (Table 2). This occurrence may contribute to depict *T. similis* as a species more adaptable to the habitat salinity variation than previously supposed, as it has recently seen in populations of *T. folliculata* and *T. kellicottiana* which were collected in brackish habitats with 2‰ and 6.5‰ salinity, respectively (Lu et al., 2018).

Considering the nature of *T. similis* as a freshwater form, it should be compared with other 11 reported freshwater congeners: *T. anomala* Xu, 1990 (The original name in Xu (1990) is *T. anomola* but it is an incorrect spelling of the species-group name according to ICZN (International Commission on Zoological Nomenclature) (1999), Article 31.2, hence, we corrected it as "*anomala*"), *T. cylindrica* Stiller, 1946, *T. folliculata* Kent, 1881, *T. incisa* (von Daday, 1910) Trueba, 1980, *T. inflata* Gong, 1989a, *T. innixa* Stokes, 1882, *T. gracilis* Sommer, 1951, *T. kellicottiana* (Stokes, 1887) Kahl, 1935, *T. qinghaiensis* Gong, 1989b, *T. scupulosus* Li et Li, and *T. vasiformis* Hammann, 1952 (Lu et al., 2018; Trueba, 1980).

From the comparison shown in Table 2, most congeners can be clearly distinguished from *T. similis* based on the general morphology, e.g., according to lorica shape and stalk length, excepting *T. folliculata* and *T. kellicottiana*. Indeed, these three species share the presence of a nearly cylindrical lorica with its posterior part tapering towards the base and no distinct ornamentations, and of a conspicuous inner stalk. Furthermore, all these three species have a similar body and lorica size. According to the oral ciliature data on *T. folliculata* and *T. kellicottiana* provided by Lu et al. (2018) and to our result on *T. similis*, this feature is basically congruent among the three species and cannot be used for species discrimination. Summarizing all morphological documentations available on these three similar species, we agree with previous authors that *T. similis* differs from *T. folliculata* and *T. kellicottiana* in the following features: (1) habitat (unique sewage habitat in *T. similis* vs. fresh or brackish water in *T. folliculata* and *T. kellicottiana*); (2) undulating lorica (frequently reported in *T. similis* vs. not mentioned for the other two species); (3) stalk length (usually shorter than 10 μm in *T. similis* vs. usually longer than 10 μm in *T. folliculata*); (4) the widest part of the lorica when viewed from the wide side (at mid-point in *T. similis* vs. at aperture in *T. folliculata*); and (5) number of valves (one in *T. similis* vs. two in some populations of *T.*

folliculata and *T. kellicottiana*) (Bock, 1963; Foissner et al., 1992; Lu et al., 2018; Trueba, 1980). The Chinese population of *T. kellicottiana* resembles *T. similis* based on its inner stalk length, but they can still be distinguished by the number of valve (two in *T. kellicottiana* vs. one in *T. similis*) (Lu et al., 2018). Based on these taxonomic emendations, some previous records of *T. kellicottiana* reported during investigations on protozoan community in activated sludge systems, such as Dubber and Gray (2011a, 2011b) and Babko et al. (2014), should be considered as misidentifications, despite the lack of detailed morphological descriptions.

4.2. TEM observation

Few ultrastructural studies have been performed on peritrich ciliates (e.g., Bauer-Nebelsick et al., 1996; Bradbury, 1965; Couch, 1973; Eperon, 1985; Eperon and Grain, 1983; Fish and Goodwin, 1976; González, 1978, 1979; Guinea et al., 1990; Lom and Corliss, 1968; McKanna, 1973; Ruiz and Anadon, 1988; Warren, 1983); as for the family Vaginicolidae, ultrastructural features have been studied in detail only for *Thuricola folliculata* and *Platycola decumbens* (Eperon, 1985; Eperon and Grain, 1983; González, 1978, 1979; Warren, 1983). Thus, there are only few ultrastructure references to make a comparison with our data on *T. similis*, and similar multimethod studies on peritrichs with ultrastructural investigations are urgently needed to better understand the biodiversity and systematics of these ciliates.

TEM observations revealed that the fibrous nature of the lorica of *T. similis* (Fig. 5C) is consistent with González (1978, 1979)'s analysis on the lorica of *T. folliculata*, and similar to the lorica of *P. decumbens* revealed by Warren (1983). Our SEM observations showed that the external surface of *T. similis* lorica wall has no decorations (Figs. 4A,B), whereas it is decorated with striations and numerous small spheres in *P. decumbens* (Warren, 1983).

The zooid of *T. similis* is bound by a pellicle whose structure is essentially similar to other sessile peritrichs (Bauer-Nebelsick et al., 1996; Carey and Warren, 1983; Eperon, 1985; González, 1978; Kawamura, 1973; Lom and Corliss, 1968; Ruiz and Anadon, 1988). However, compared with the conspicuous rounded alveoli in *T. folliculata* (Eperon and Grain, 1983; González, 1978, 1979) and the distinct concave alveoli in *P. decumbens* (Warren, 1983), the alveolar pattern of *T. similis* is different, being a thin, non-prominent space (Fig. 6A). Nothing is known concerning alveolar content.

The arrangement of the peristomial ciliature of *T. similis* generally corresponds to that of other known peritrichs (Bradbury, 1965; Lom and Corliss, 1968; Rosenberg and Grim, 1966), in which the haplokinety (composed of a ciliferous plus an aciliferous kinetosome row) is located upper with respect to the polykinety (composed of three ciliferous rows), and separated by an ectoplasmic ridge.

A single postciliary microtubule on the left side of the aciliferous row of the haplokinety was observed in *T. similis* (Fig. 6F), whereas two postciliary microtubules were present at the same position in *T. folliculata* during final stage of binary fission (Eperon and Grain, 1983). As for the polykinety ultrastructure, a similar arrangement was observed in our *T. similis* and *T. folliculata* (Eperon and Grain, 1983), i.e., the presence of a long fibrillar band running posteriorly along each kinetosome of the left row, and a connection structure between the kinetosomes of the same row (Figs. 6G,H). However, in *T. similis*, the dense material that connect the kinetosomes is restricted to its base (see the asterisks in Fig. 6G), and envelops two microtubules, whereas, in Eperon and Grain (1983), no microtubules were detected and the connection material appeared less electrodense due to the more superficial section level.

4.3. Mitochondrial genome

Ciliates' mitochondrial genomes are known to possess several peculiar features and that of *Thuricola similis* does not break this paradigm. Indeed, its mitochondrial genome (1) was identified as linear; (2) possessed protein coding and tRNAs genes shared by all ciliate mitochondrial genomes; and (3) showed several split genes such as *nadh1*, *rnl*, and *rpS3* (Barth and Berendonk, 2011; Burger et al., 2000; de Graaf et al., 2009; Gao et al., 2018; Li et al., 2018; Moradian et al., 2007; Park et al., 2019a; Pritchard et al., 1990; Schnare et al., 1986; Serra et al., 2020; Suyama and Miura, 1968; Swart et al., 2012). However, in *T. similis*, only some of the fragments of these three split genes were retrieved, i.e., *nadh1*_a, *rnl*_b, and *rpS3*_b. In our opinion, the apparent absence of *nadh1*_b, *rnl*_a, and *rpS3*_a is due neither to the incompleteness of the sequenced genome nor to the real absence of these gene fragments, but to their high divergence making them at present undetected by BLAST analysis or prediction software. Presumably, this gap will be filled as soon as more and more complete genome sequences of representatives of the class Oligohymenophorea will be available.

A surprising feature found in the mitochondrial genome of *T. similis* lays in its gene organization: the predicted direction of the transcription goes away from a central region constituted of A-T rich repeated units. This organization has not been found in any other oligohymenophorean congener (Barth and Berendonk, 2011; Burger et al., 2000; de Graaf et al., 2009; Moradian et al., 2007), but the same or a similar structure has been disclosed in ciliates belonging to the class Spirotrichea (de Graaf et al., 2009; Serra et al., 2020; Swart et al., 2012). Unfortunately, since the present work is the first work providing a complete mitochondrial genome in the subclass Peritrichia, it is impossible to determine whether all peritrichs share such organization or not. In addition, the true function of the central region needs further investigation.

Lastly, the presence of nearly half of unclassified ORFs may either suggest that the metabolic capability of *T. similis*'s mitochondria is more complex than expected, or that a high evolutionary rate for these mitochondrial genes does not allow us to properly identify homologous of already known genes.

4.4. Phylogenetic position

In comparison with aloricate sessilids, rather less sequences of loricate peritrichs are available in the GenBank. In the last two decades, about 13 18S rRNA gene sequences of Vaginicolidae family along with the sole sequence of Usconophryidae family have been deposited in GenBank (Dunthorn et al., 2012; Lu et al., 2018; Lu et al., 2019; Miao et al., 2004; Sun et al., 2016; Zhuang et al., 2016). Among them, nine were identified at species level, namely *Cothurnia annulata*, *C. ceramicola*, *C. salina*, *Pyxicola pusilla*, *Thuricola folliculata*, *T. kellicottiana*, *T. obconica*, *Vaginicola crystallina*, and *V. tincta*. However, there were no specific morphological reports for *C. annulata* and *V. crystallina*. Apart from that, an unidentified *Vaginicola* sp. KJ649621 was also recorded in GenBank from an unpublished paper. The present study included in the phylogenetic analyses all those above-mentioned 15 sequences, two newly obtained sequences of *T. similis*, as well as two highly correlated, relatively long environmental sequences (AB901620, LC150077).

In both ML and BI trees, as expected, *T. similis* clustered with congeners within the family Vaginicolidae (Fig. 9), although the phylogenetic relationships among *Thuricola* species were still unclear. Our study is consistent with previous work (Lu et al., 2018) where *Vaginicola* sp. KU363269 always clustered with *Thuricola* species and then grouped with *Vaginicola* sp. KU363258, *V. crystallina* AF401521, and *Vaginicola* sp. KU363266. In the present work, the first

introduced environmental sequence, namely the uncultured eukaryotes AB901620, was proved to be conspecific of *Vaginicola* sp. KU363269, as they were identical to each other via BLAST, even though their habitats were rather different: AB901620 was sampled in the municipal WWTP in Japan, whereas KU363269 was found in the coastal region of Maryland in USA (Matsunaga et al., 2014; Sun et al., 2016). Moreover, looking at the distribution of all *Vaginicola* species throughout the phylogenetic tree (Fig. 9), we find that (1) some of them, as mentioned before, are clustering with *Thuricola* species; (2) *Vaginicola* sp. KJ649621 is always nesting within *Cothurnia* genus (Lu et al., 2018; Sun et al., 2016); (3) *V. tincta* is located far away from other congeners and clusters with *Usconophrys* sp., together forming a sister clade to *Pyxicola-Cothurnia* assembly.

However, compared with other *Vaginicola* spp., the position of *V. tincta* in the present work seems not reliable although supported by a high branch value. Indeed, it has already been reported by previous works that the phylogenetic position of *Usconophrys* sp. differs among trees constructed using different sequences and different analysis methods (Lu et al., 2018; Sun et al., 2016). Additionally, *V. tincta* differs from *Usconophrys* sp. not only in morphology (i.e., Usconophryidae possess a hemispherical or urn-shaped lorica and opercullariform peristome, while Vaginicolidae has a conical to cylindroid lorica and an epistyliform peristome), but also in according to molecular marker analysis (*Usconophrys* sp. JQ723986 only shares about 88.94% similarity with *V. tincta* MK184557) (Clamp, 1991; Lynn, 2008 and Supplementary Table S1). Long branch attraction is the probable reason for the clustering of *V. tincta* and *Usconophrys* sp. in our phylogenetic reconstruction; moreover, we think that the real systematic relationship between these two species, or even between Usconophryidae and Vaginicolidae families, has not yet been resolved mainly due to the paucity of sequence data.

Besides, among all *Vaginicola* species, *V. tincta* is the only one for which a detailed morphological description has been published jointly with the 18S rDNA sequence (Lu et al., 2019). Hence, it is reasonable to distrust the classification as putative *Vaginicola* spp. for other available sequences: they might be *Thuricola*'s or *Cothurnia*'s sequences, since these two genera and *Vaginicola* are morphologically hardly distinguishable (Lu et al., 2018; Trueba, 1980; Warren and Paynter, 1991). Therefore, based on our findings and literature data, we hypothesize that: (1) *Vaginicola* sp. KU363269, conspecific to the uncultured eukaryotes AB901620, is a representative of *Thuricola*, since both of them are identical in 18S rDNA sequencing and robustly nested within the genus (Lu et al., 2018 and Fig. 9); in addition, the uncultured eukaryotes AB901620 shares a relative high similarity (98.18–98.52%) with other known *Thuricola* species (Supplementary Table S1); (2) Similarly, uncultured eukaryote LC150077 and *Vaginicola* sp. KJ649621 are in reality two *Cothurnia* species (Lu et al., 2018 and Supplementary Table S1); (3) The identification of the rest putative *Vaginicola* species, namely *Vaginicola* sp. KU363258, *V. crystallina* AF401521, and *Vaginicola* sp. KU363266, should still be considered questionable: as they branch basally to *Thuricola* clade, any speculation with the present data would be hasty (Lu et al., 2018; Lu et al., 2019 and Fig. 9). Therefore, while both *Cothurnia* and *Thuricola* genera appear monophyletic, based on the split between *V. tincta* and those questionable *Vaginicola* species, *Vaginicola* very likely represents a polyphyletic genus.

In conclusion, it is difficult to determine the phylogenetic relationships among/within families and genera of loricate sessilids because relatively few representatives of these taxa have been sequenced so far. Moreover, among the available sequences of loricate representatives, several of them are not taxonomically verified yet, which unfortunately further reduces the reliability of these sequences.

4.5. Phylogenomic analyses and evolutionary relationships among Oligohymenophorea subclasses

The evolutionary relationships among the subclasses of Oligohymenophorea, i.e., Hymenostomatia, Peniculia, Peritrichia, and Scuticociliatia, have been increasingly debated, since their phylogenetic positions are unstable both in works based on 18S rDNA phylogenies (e.g., Li et al., 2006; Miao et al., 2004; Miao et al., 2001; Strüder-Kypke et al., 2000; Utz and Eizirik, 2007; Utz et al., 2010) and concatenated rDNA sequences phylogenetic analyses (e.g., Gao et al., 2013; Gao et al., 2016). Phylogenomic analyses have been proved to generally improve the robustness of molecular phylogenetic reconstructions, untangling many previously debated phylogenies in various taxa (Feng et al., 2015; Gentekaki et al., 2014; Gentekaki et al., 2017; Jiang et al., 2019; Lasek-Nesselquist and Johnson, 2019; Lynn and Kolisko, 2017; Lynn et al., 2018; Pan et al., 2019; Sheng et al., 2018; Sun et al., 2017b; Wang et al., 2019). Until now, there are only a few phylogenomic analyses on the class Oligohymenophorea and all of them use nuclear gene datasets. In these studies, the subclass Peritrichia was positioned either as a sister clade to Peniculia (Feng et al., 2015; Jiang et al., 2019) or in a basal position within the class Oligohymenophorea (Gentekaki et al., 2017; Pan et al., 2019). Our phylogenomic trees obtained from an independent mitochondrial gene dataset using ML and BI methods, corroborate the topology retrieved by Gentekaki et al. (2017) and Pan et al. (2019) which supports the Peritrichia as a sister group to all remaining Oligohymenophorea subclasses. Moreover, this topology has been proven to be the most robust through topology test. However, the sisterhood between Peritrichia and Peniculia could not be fully rejected (see Fig. 11).

Our finding that the subclass Peritrichia branches far away from other subclasses is coherent with the old morphological classification system of ciliates proposed by Corliss (1979) where Oligohymenophorea class was only divided into two subclasses, Hymenostomata and Peritricha. The former, at that time including scuticociliates and peniculian species, was clearly distinguished from the latter in many aspects: (1) body shape (pyriform to elongate-ovoid vs. inverted bell-like or goblet-like or conical-cylindrical); (2) organization of oral apparatus (inconspicuous, composed of a dikinetid paroral and several polykinetid membranelles or the peniculi vs. conspicuous, composed of a paroral and oral polykinetids, both encircling the apical end in a counterclockwise sense before entering the oral infundibulum); (3) somatic ciliature (typically holotrichous vs. reduced to trochal band, which is permanently ciliated on mobile species and temporarily ciliated on the telotroch of sessile species); and (4) life style (free swimming vs. most sessile and sedentary) (Corliss, 1979; Lynn, 2008).

Another hint of the plausible early branching of *T. similis* (as representative of the Peritrichia subclass) in Oligohymenophorea may derive from the organization of its mitochondrial genome. Indeed, *T. similis*'s mitochondrial genome shows a central region (where ORFs started to transcribe in both directions) with A-T rich tandem repeats, which is somehow similar to those observed in Spirotrichea mitochondria but not present in other oligohymenophorean ciliates (Barth and Berendonk, 2011; Burger et al., 2000; de Graaf et al., 2009; Gao et al., 2018; Li et al., 2018; Moradian et al., 2007; Park et al., 2019a; Serra et al., 2020; Swart et al., 2012 and Fig. 10). Alike *T. similis*, the structure of central region of mitochondrial genomes of three *Euplotes* species, namely *E. minuta*, *E. crassus*, and *E. vanleeuwenhoeki*, consists of tandemly repeated A-T rich, 16–18 nt units (de Graaf et al., 2009; Serra et al., 2020). Also, the A-T rich central region can be found in other hypotrichs' mitochondrial genomes, namely *Oxytricha trifallax*, *Laurentiella strenua*, and *Pseudourostyla cristata*, but the above mentioned tandemly repeated units are hardly to be recognized (Park et al., 2019a; Swart et al., 2012). Further investigation are needed to assess whether the presence of an A-T rich central region in mitochondrial genome is (1) an ancestral

feature of the subphylum Intramacronucleata, but subsequently lost by the ancestor of subclasses Peniculia, Scuticociliatia, and Hymenostomatia; or (2) a result of convergent evolution in mitochondrial chromosome organization between *T. similis* and the class Spirotrichea.

Unfortunately, the lack of complete mitochondrial genome sequences for most ciliophoran classes at present precludes the possibility of testing these two hypotheses.

To sum up, starting from a rigorous integrative taxonomic redescription of two far away located populations of the little-known peritrichous species *T. similis*, in line with the "Next Generation Taxonomy" approach proposed by Serra et al. (2020), we have been able to contribute in providing answers to a more general evolutionary problem such as the disentangling of phylogenetic relationships among subclasses of Oligohymenophorea. We strongly believe that the introduction of complete mitochondrial genome sequencing in the description of novel species and/or the redescription of known species, will significantly contribute to solving evolutionary relationships within Ciliophora phylum in the next future.

4.6. Neotypification of *Thuricola similis* Bock, 1963 based on the Italian population

4.6.1. Neotype material and locality

Considering the incompleteness of the original and the subsequent descriptions on *Thuricola similis* (see Table 2), and according to items (1), (2), (4), and (6) listed in the chapter 2.4.2 by Foissner et al. (2002), it needs neotypification. We designate the Italian population as a neotype of *T. similis* because: (1) the neotype is morphologically similar to the original German population described by Bock (1963) (Table 2); (2) More data concerning the ciliature come from protargol stained specimens of Italian population than from the Brazilian one; (3) Although the 18S rRNA gene sequencing was performed on specimens from both populations, mitochondrial genome assembly and annotation was performed only on Italian population; (4) Compared with the Brazilian one, Italian population is geographically closer to the original description, i.e., they both come from European continent. Thus, the neotype locality is Cuoiodepur WWTP in San Romano (Pisa), Italy (43°41'44.5"N, 10°46'02.7"E) (see the above section "2.1." for more details). Data from all so far studied *T. similis* populations are used for the emended diagnosis, while some supplementary observations are provided from the neotype population.

4.6.2. Type material

Two protargol-stained slides (registration number-srn: CAMUS_2020-6, -7) and one permanent Feulgen-stained slide (srn: CAMUS_2020-8) have been deposited in the collection of the Museo di Storia Naturale e del Territorio dell'Università di Pisa (Calci, Pisa, Italy). Two additional slides, one protargol-stained slide (srn: Unipi_2020-4) and one permanent Feulgen-stained slide (srn: Unipi_2020-5), have been deposited in the collection of the Unit of Zoology-Anthropology of the Department of Biology at University of Pisa (Pisa, Italy). Furthermore, one voucher slide with protargol-stained specimens of the Brazilian population (srn: IBZ-UFRJ0016-6) has been deposited in the collection of Laboratório de Protistologia, Universidade Federal do Rio de Janeiro (Rio de Janeiro, Brazil). Neotypes and other relevant specimens were marked by a blue ink circle on the coverslip.

4.6.3. Gene sequence

The 18S rRNA gene sequence and the complete mitochondrial genome of *Thuricola similis* (neotype population) have been deposited in NCBI GenBank database with the accession numbers

MW208818 and MW221262, respectively. The accession number of the 18S rRNA gene sequence of the Brazilian population is MH120840.

4.6.4. Emended diagnosis

Zooid 136–314 × 9–36 µm *in vivo*, trumpet-shaped with enlarged anterior region and posterior region tapering towards the stalk. Inner stalk 7–22 µm long, usually more than 10 µm. Lorica 139–250 µm long, roughly cylinder-shaped with posterior third to fourth of lorica gradually tapered. Lorica nearly symmetrical on wide side and asymmetrical on narrow side with a neck at the upper third; lorica aperture elliptical. Irregular small undulations in lorica wall present in some individuals. A single valve located nearly in the upper third to fourth of lorica. In total, approximately 136–232 transverse striations encircling the zooid body. Oral ciliature typical of the genus. Sewage species found in fresh and brackish water.

Acknowledgements

This work was supported by the European Commission FP7-PEOPLE-2009-IRSES project CINAR PATHOBACTER (247658) (to G.P.); the University of Pisa PRA_2018_63 project (to G. P.); the Ministry of Foreign Affairs and International Cooperation Scholarships Protocol ID:1559731487 (to W.L.); Conselho Nacional de Desenvolvimento Científico e Tecnológico (CNPq) 140627/2019-7 (to P.H.C.-N), 140896/2015-5 (to R.deO.M), 437655/2018-0 (to T.daS.P), and 311577/2019-9 (to I.D.S.-N.).

Great thanks to the Consorzio Cuoiodepur, for providing the sampling materials, in particular to Dr. Gualtiero Mori and Dr. Francesco Spennati. Special acknowledgements to Mr. Simone Gabrielli for his kind help for SEM preparation and observation and to Dr. Cristiana Sigona for her isolation and long-term cultivation of the Italian population of *T. similis*. We are also grateful to Marcelo Sales for his technical support, and to Dr. Roberto Júnio Pedroso Dias for assisting in the DNA sequencing of the *T. similis* Brazilian population.

Appendix A. Supplementary material

Supplementary data to this article can be found online at XXXXXXXXXX.

Table 1. Morphometric data on two populations of *Thuricola similis* from WWTPs (a, Brazilian population, first line; b, Italian population, neotype, second line). CV, coefficient of variation in %; M, mean; Max, maximum value; Min, minimum value; N, number of specimens; No., number; SD, standard deviation; TB, trochal band. All data are based on live specimens and measurements are given in micrometer.

Characters	Min	Max	M	SD	CV	N
Zooid length[a, b]	211	314	249.0	26.0	10.0	25
	136	274	192.5	37.3	19.4	27
Zooid width at midpoint[a, b]	14	19	16.9	2.0	11.9	10
	9	19	13.4	2.6	19.8	27
Peristomial collar width[a, b]	21	32	27.4	2.1	7.7	25
	25	41	33.0	3.6	10.8	22
Peristomial collar thickness[a]	5	8	5.8	0.6	9.9	25
Peristomial disc width[a]	18	28	21.5	2.6	12.0	25
Infundibulum length[a, b]	33	48	38.8	3.2	10.3	25

	30	44	38.3	4.7	12.2	12
Lorica length[a, b]	157	210	186.3	12.0	6.5	25
	139	194	172.9	14.8	8.6	14
Lorica width at midpoint from wide side[a, b]	40	49	44.3	2.5	5.6	25
	42	50	44.7	3.6	8.1	4
Lorica width at midpoint from narrow side[b]	36	58	43.4	7.6	17.5	10
Aperture width from wide side[a, b]	28	47	37.4	5.8	15.4	25
	38	47	41.4	5.1	12.3	3
Aperture width from narrow side[b]	26	55	33.8	9.1	27.0	10
Lorica width at base from width side[a, b]	13	19	15.8	1.8	11.6	25
	13	18	15.5	2.1	13.7	3
Lorica width at base from narrow side[b]	10	14	12.1	1.5	12.7	5
Stalk length[a, b]	8	22	14	3.2	22.0	25
	7	18	11.8	3.3	27.9	13
Stalk width[a]	2	4	2.8	0.5	20.1	25
Length of valve[a, b]	31	42	36.0	3.9	10.8	18
	31	46	36.6	4.5	12.3	9
No. of striations from peristome to TB[b]	83	117	97.7	10.7	10.9	11
No. of striations from TB to scopula[b]	80	94	87.0	4.1	4.7	11
No. of striations (in total)[a, b]	136	232	183.6	30.9	16.8	9
	169	203	184.7	11.1	6.0	11
Contractile vacuole width[a, b]	12	19	16.2	1.5	9.7	25
	12	19	16.0	2.3	14.2	10
Food vacuole width[a, b]	5	13	9.1	2.1	23.6	24
	3	13	6.1	2.5	40.1	22

Table 2. Morphological comparison among populations of *Thuricola similis* and freshwater congeners. a, with a small secondary valve but overlooked, according to Lu et al. (2018). NA, not available; No., number; S, salinity; X, mean value. Bold fonts highlight the distinct differences among *T. similis* and other congeners.

Species	Zooid size (μm)	Lorica length (μm)	Lorica width at midpoint (μm)	Aperture width (μm)	Stalk length (μm)	Lorica shape	No. of valve	Habitat	Data source
T. similis (Brazilian population)	211–314 × 14–19 (X = 249 × 17)	157–210 (X = 186)	40–49 (X = 44.3)	28–47 (X = 37.4)	8–22 (X = 14)	Cylindrical, tapering towards the base; widest diameter in the lower half and occasionally with soft undulations	1	WWTP, S = 0.41‰	This work
T. similis (Italian population, neotype)	136–274 × 9–19 (X = 193 × 13)	139–194 (X = 173)	36–58 (X = 43.8)	26–55 (X = 35.5)	7–18 (X = 11.8)	Cylindrical, tapering towards the base; nearly symmetrical on the wide side with irregular undulations while asymmetrical on the narrow side with anterior third narrower and neck-like; widest on the middle portion	1, sometimes with spine	WWTP, S = 0–10‰	This work
T. similis (original population)	220–290 long (X = 250)	158–248 (X = 183)	40–49 (X = 45)	45	10–20 (X = 14)	Cylindrical, tapering towards the base; lorica wall not smooth but somehow with undulations	1	WWTP, S = 0‰	Bock (1963)
T. similis (Ukrainian population)	192–270 × 15–36	150–250	39–54	NA	NA	NA	1	WWTP, S = 0‰	Konstantynenko (2007)
T. kellicottiana	180–435 ×20–35	160–290	40–75	27–65	4–50, usually less than 25	Nearly symmetrical on the wide and asymmetrical on the narrow side; anterior third inclined with convexity under aperture on the valve side, posterior	**1[a] or 2, with a spine**	Freshwater or brackish (S = 6.5‰)	Lu et al. (2018)

						portion tapering towards base with two annular bulges to form a long, slender rear; widest diameter in the lower half			
T. folliculata	165–420 ×15–27	125–300	39–75	32–75	**Usually less than 10**	Viewed from the wide side, nearly symmetrical, **slightly widened towards the front, with the widest diameter at the aperture;** viewed from the narrow side, asymmetrical, with a neck at the upper 1/3	**1[a] or 2**	Freshwater or brackish (S = 2‰)	Lu et al. (2018)
T. innixa	145–190 ×18–27	110–200	30–52	30–35	**Short or absent**	Cylindrical, **rounded at its base**	**2**	Freshwater	Kahl (1935); Shen and Gu (2016); Trueba (1980)
T. gracilis	144–290 ×16–25	100–195	38–52	21–32	**Short or absent**	**Rounded at its base;** tapering towards a bottleneck near the aperture when viewed from the narrow side, with the widest diameter near the base; tapering slightly towards the base and looking rectangular when viewed from the wide side	1	Freshwater	Sommer (1951)
T. incisa	NA	160–180	NA	NA	**Short**	Edge of aperture vertically indented; **rounded at its base; inferior part inflated**	1	Freshwater	Trueba (1980)
T. vasiformis	178–215 × 20–23	110–160	38–59	25	**Short or absent**	**Widest diameter at the base; resembling a small Erlenmeyer bottle**	1	Freshwater	Shen and Gu (2016); Trueba (1980)

T. cylindrica	137–172 long	148	41	25	**Short**	Anterior part narrowing, posterior 1/3 widening **with rear end rounded**	1	Freshwater	Shen and Gu (2016)
T. anomala	225–235 ×23–27	140–160	42–48	26–29	**Short**	**With an oblique neck**	1	Freshwater	Xu (1990)
T. inflata	130–150 long	**72–76**	31–34	25–27	**Short**	Front view, **tube-like**; with several shallow undulations present in the lateral margin; **rounded at the base**	1	Freshwater	Gong (1989a)
T. qinghaiensis	149–160 long	**120–136**	**10–54**	**10–12**	**Short**	**Elongate tube-shaped;** from narrow side, 1/3 anterior portion narrowing; **rounded at the base**	1	Freshwater	Gong (1989b)
T. scupulosus	224–240 × 28–30	120–145	50–60	NA	**Short or absent**	Cylindrical, with **the edge of aperture jagged**	1	Freshwater	Shen and Gu (2016)

Fig. 1. Schematic line drawings illustrating *Thuricola similis in vivo* (A–F) and after protargol staining (G,H). (A,B) Wide (A) and narrow (B) side views respectively of two loricae bearing a single zooid each. In (B) arrow indicates a bulge. (C,D) Wide side views on loricae bearing two zooids (C) and a single zooid (D), respectively; in (D) arrows indicate small undulations decorating the lorica and arrowheads point to filamentous bacteria. (E) Narrow side view of an individual with two contracted zooids. (F) Narrow side view of an empty lorica with a fine spine in the valve. (G) Nuclear apparatuses. (H) Tentative reconstruction of the whole cell ciliature based on the silver stained specimen whose infundibular portion is presented in Fig. 3A and some oral infraciliature features in common among sessile peritrichs. Black and gray line drawings represent structures present in opposite planes. Due to heavy staining of some areas of the specimen, the detailed kinetosomal arrangement of epistomial membrane 1 and 2, germinal kinety, and trochal band is unclear, thus only their relative positions, orientations, and kinetosomal numbers are depicted. Additionally, in the peristomial area, the three rows of kinetosomes of the polykinety and the two rows of the haplokinety have been simplified. Dash lines in the first inflection point of infundibular polykinety 1 and 2 indicate the rational correct directions (according to Lu et al. (2018) and specimens presented in Figs. 3F,G) of the three rows of kinetosomes respectively included by each of them. Asf, activated sludge floccule; CV, contractile vacuole; EM1, 2, epistomial membrane 1, 2; FV, food vacuole; G, germinal kinety; H, haplokinety; Inf, oral infundibulum; JM, junctional membrane; LB, lorica base; Ma, macronucleus; Mi, micronucleus; P1–3, infundibular polykinety 1–3; Pc, peristomial collar; Pd, peristomial disc; Po, polykinety; Sc, scopula; Sp, spine; St, stalk; TB, trochal band; Val, valve. Scale bars: 80 μm.

Fig. 2. *In vivo* photomicrographs of *Thuricola similis*. (A,B) Wide side views of two individuals with one and two zooids, respectively. (C) Lorica bearing a single zooid attached to a conspecific' s lorica where three contracted zooids living together. Arrow indicates a bulge above the valve position from the narrow side view; arrowheads indicate some small undulations of the lorica. (D) Three relaxed anisometric zooids sharing the same lorica. (E) Wide side view of an individual with a single zooid. Arrowheads indicate small undulations on the lorica wall. (F) Narrow side view of an individual with two zooids. (G) A special individual with a microconjugant (arrow) and a normal zooid inside the lorica. (H) The anterior portion of zooid showing single-layered peristomial collar. Arrow points to the contractile vacuole. (I) Closer view to show striations of pellicle near trochal band. (J) Two aloricate zooids. (K) Lorica with two zooids attached to an empty conspecific's lorica with many activated sludge floccules inside and outside. (L) Narrow side view of an empty lorica showing a fine spine in the valve. (M) An individual with a contracted zooid. (N) Enlargement of the posterior portion: junctional membrane, scopula, and stalk are visible. Arrowheads indicate the extended lorica base. FV, food vacuole; Inf, oral infundibulum; JM, junctional membrane; Pc, peristomial collar; Pd, peristomial disc; Sc, scopula; Sp, spine; St, stalk; TB, trochal band; Val, valve. Scale bars: 100 μm.

Fig. 3. Photomicrographs of *Thuricola similis* after protargol staining according to Foissner (1992b) (A–G) and Dieckmann (1995) (H,I). (A) Ciliature of the infundibular portion. (B) Partial ciliature around peristome showing epistomial membrane 1 and 2. Asterisk indicates the starting point of haplokinety and polykinety. (C) Detail of the polykinety in the peristomial area showing it is composed of three rows of kinetosomes (black circles). (D) A stained specimen showing basal bodies in trochal band and scopula (arrow). (E,F) Detail of ciliature in the infundibular area where haplokinety is composed of two kinetosomes (E) and infundibular polykinety 1 to 3 are composed of three kinetosomes (F). Row 2 and 3 of the infundibular polykinety 3 are hard to be distinguished due to overlapping. Arrow and arrowhead in (F) respectively indicate the abstomally diverged row 3 of the infundibular polykinety 2, and the longer row 1 of the infundibular polykinety 3. (G) Details of three infundibular polykineties in another specimen where abstomal portion of infundibular

polykinety 3 is not visible. Arrow indicates row 3 of the infundibular polykinety 2 abstomally diverging from the other two rows. (H,I) Nuclear apparatus showing macronucleus and micronucleus. EM1, 2, epistomial membrane 1, 2; G, germinal kinety; H, haplokinety; Ma, macronucleus; Mi, micronucleus; P1–3, infundibular polykinety 1–3; Po, polykinety; TB, trochal band. Scale bars: 30 µm.

Fig. 4. Scanning electron micrographs of *Thuricola similis.* (A,B) Loricae with some debris/rod bacterium (arrowheads) and filamentous bacterium (arrows) on the surface. (C) A partially contracted stalked zooid form: two zooids share the stalk. The zooid surface is highlighted by pellicular striations. (D,E) Enlarged images of the surface of the stalked zooid in Fig. 4C, respectively showing the anterior portion (D) and the portion near to the telotroch band (E). About 20 convoluted rows of striations measured from peristomial collar are recognizable in (D) and the telotroch band composed of four closely spaced specialized striations can be clearly seen in (E). C, cilium; St, stalk; TB, trochal band. Scale bars: 50 µm (A,B), 20 µm (C), 5 µm (D), and 2.5 µm (E).

Fig. 5. Transmission electron micrographs of the Brazilian population of *Thuricola similis.* (A) General view of the peristome in a transversal section showing its ciliature composed by the haplokinety (only one ciliary row is visible) and the polykinety (three ciliary rows). (B) Deeper and slightly oblique section through the peristome. (C,D) Details of the haplokinety and polykinety in two oblique sections. The first and second laps of the haplokinety and polykinety are visible in (C), as well as an ectoplasmic ridge separating the haplokinety from the polykinety. The haplokinety presents two rows of basal bodies, but only the most external row is ciliferous. The polykinety presents three ciliferous rows. Several bacteria used as food source are visible. AR, aciliferous row; Ba, bacteria; CR, ciliferous row; ER, ectoplasmic ridge; H, haplokinety; L, lorica; M, macronucleus; Mit, mitochondria; OC, oral ciliature; OR, oral ribs; P, polykinety; P1–3, infundibular polykinety 1–3; Pe, peristome. Magnification: 3,000× (A), 5,000× (B), 10,000× (C), and 15,000× (D).

Fig. 6. Transmission electron micrographs of the Brazilian population of *Thuricola similis.* (A) Cortex in a slightly oblique section. (B) Transverse section showing the well-developed myonemal layer on the peristomial collar, and lorica. (C) Detail of the lorica in Fig. 6B showing its amorphous microfibrillar material, probably of protein origin. (D,E) Oblique section of the cytostome showing the oral ribs. Arrowheads in (E) show the microtubules strengthening the oral ribs. (F) Detail of the haplokinety. The basal bodies of the aciliferous row show only one postciliary microtubule. (G,H) Detail of the polykinety. Asterisks in (G) indicate the absence of dense material between kinetosomes in the most superficial area of the oblique section. Arrowheads in (H) indicate basal microtubules in the polykinety bases. AL, alveolar layer; AR, aciliferous row; CR, ciliferous row; DM, dense material; Ep, epiplasm; ER, ectoplasmic ridge; FB, fibrillar band; H, haplokinety; L, lorica; ML, myonemal layer; MM, microfibrillar material; OC, oral ciliature; OR, oral ribs; PC, peristomial collar; Pc, postciliary microtubule; PM, plasma membrane. Magnification: 25,000× (A), 8,000× (B), 40,000× (C,F–H), and 20,000× (D,E).

Fig. 7. Transmission electron micrographs of the Brazilian population of *Thuricola similis.* (A,B) Endoplasm in oblique section showing mitochondria and endosymbiotic bacteria in longitudinal and cross section. (C) Endosymbiotic bacteria near to mitochondria at a higher magnification. (D) Endosymbiotic bacteria during binary fission. EB, endosymbiotic bacteria; Mit, mitochondria; H, haplokinety. Magnification: 30,000× (A,B), 50,000× (C), and 12,000× (D).

Fig. 8. Mitochondrial gene map of *Thuricola similis*. Names of split genes are suffixed by _a and _b. tRNAs are indicated by a single letter according to amino acid codon table. The directions of transcription are indicated by light blue arrows.

Fig. 9. Phylogenetic tree inferred from 18S rRNA gene sequences, revealing the phylogenetic position of *Thuricola similis* (both Brazilian and Italian populations, bold fonts). Numbers near nodes are bootstrap values for ML and posterior probabilities for BI, respectively. Accession numbers are provided after species names. Black dots indicate nodes with full support in both analyses, red triangles indicate species with clear taxonomic data within Vaginicolidae family. Clades with a different topology in the BI tree are shown by asterisks. The scale bar indicates five substitutions per 100 nucleotides. Systematic classification follows Lynn (2008).

Fig. 10. Phylogenomic tree of *Thuricola similis* (in big and bold font) inferred from a concatenated amino acid sequences alignment of 20 selected mitochondrial protein coding genes (for details see Supplementary Table S2), with all selected species' corresponding mitochondrial gene maps inserted where ORFs are shown in blocks with orange and black representing left and right directions of transcription. Numbers associated to nodes represent bootstrap values for ML and posterior probabilities for BI, respectively. The scale bar (0.2) denotes mean number of substitutions per site.

Fig. 11. Alternative phylogenomic hypotheses based on random positioning of *Thuricola similis* inside the class Oligohymenophorea. Four hypotheses (H1–H4) are presented where H4 corresponds to the ML tree (Fig. 10) retrieved from our mitochondrial based phylogenomic analysis. *T. similis* is highlighted in red colour in four alternative hypothetical topologies. A series of statistical data for topology test of all alternative hypotheses is shown on the bottom where "+" denotes the 95% confidence set (in bold) and "-" denotes significant exclusion. logL, log-likelihood; deltaL, logL difference from the maximal logL in the set; bp-RELL, bootstrap proportion using RELL method; p-KH, p-value of one sided Kishino-Hasegawa test; p-SH, p-value of Shimodaira-Hasegawa test; p-WKH, p-value of weighted KH test; p-WSH, p-value of weighted SH test; c-ELW, expected likelihood weight; p-AU, p-value of approximately unbiased test.

References

Arnaiz, O., Meyer, E., Sperling, L., 2020. ParameciumDB 2019: integrating genomic data across the genus for functional and evolutionary biology. Nucleic Acids Res. 48, D599-D605. https://doi.org/10.1093/nar/gkz948.

Babko, R., Kuzmina, T., Jaromin-Gleń, K., Bieganowski, A., 2014. Bioindication assessment of activated sludge adaptation in a lab-scale experiment. Ecol. Chem. Eng. S. 21, 605-616. https://doi.org/10.1515/eces-2014-0043.

Bae, J.S., Kim, I., Sohn, H.D., Jin, B.R., 2004. The mitochondrial genome of the firefly, *Pyrocoelia rufa*: complete DNA sequence, genome organization, and phylogenetic analysis with other insects. Mol. Phylogenet. Evol. 32, 978-985. https://doi.org/10.1016/j.ympev.2004.03.009.

Bankevich, A., Nurk, S., Antipov, D., Gurevich, A.A., Dvorkin, M., Kulikov, A.S., Lesin, V.M., Nikolenko, S.I., Pham, S., Prjibelski, A.D., Pyshkin, A.V., Sirotkin, A.V., Vyahhi, N., Tesler, G., Alekseyev, M.A., Pevzner, P.A., 2012. SPAdes: a new genome assembly algorithm and its applications to single-cell sequencing. J. Comput. Biol. 19, 455-477. https://doi.org/10.1089/cmb.2012.0021.

Barth, D., Berendonk, T.U., 2011. The mitochondrial genome sequence of the ciliate *Paramecium caudatum* reveals a shift in nucleotide composition and codon usage within the genus *Paramecium*. BMC Genom. 12, 272. https://doi.org/10.1186/1471-2164-12-272.

Barth, D., Krenek, S., Fokin, S.I., Berendonk, T.U., 2006. Intraspecific genetic variation in *Paramecium* revealed by mitochondrial cytochrome c oxidase I sequences. J. Eukaryot. Microbiol. 53, 20-25. https://doi.org/10.1111/j.1550-7408.2005.00068.x.

Bauer-Nebelsick, M., Bardele, C.F., Ott, J.A., 1996. Electron microscopic studies on *Zoothamnium niveum* (Hemprich & Ehrenberg, 1831) Ehrenberg 1838 (Oligohymenophora, Peritrichida), a ciliate with ectosymbiotic, chemoautotrophic bacteria. Eur. J. Protistol. 32, 202-215. https://doi.org/10.1016/S0932-4739(96)80020-4.

Biernacka, I., 1963. Die Protozoenfauna in Dantziger Bucht. II. Die Charakteristik der Protozoen in Untersuchten Biotopen der Seekuste. Pol. Arch. Hydrobiol. 11, 53-75.

Bock, K.J., 1952. Über die marinen Arten der Gattung *Thuricola* (Ciliata, Peritricha). Kieler Meeresforsch. 8, 227-228.

Bock, K.J., 1963. Über das Auftreten einer *Thuricola* (Ciliata, Peritricha) in Belebtschlamm. Zool. Anz. 171, 91-96.

Boscaro, V., Vannini, C., Fokin, S.I., Verni, F., Petroni, G., 2012. Characterization of "*Candidatus* Nebulobacter yamunensis" from the cytoplasm of *Euplotes aediculatus* (Ciliophora, Spirotrichea) and emended description of the family *Francisellaceae*. Syst. Appl. Microbiol. 35, 432-440. https://doi.org/10.1016/j.syapm.2012.07.003.

Bradbury, P.C., 1965. The infraciliature and argyrome of *Opisthonecta henneguyi* Faureé-Fremiet. J. Protozool. 12, 345-363. https://doi.org/10.1111/j.1550-7408.1965.tb03226.x.

Brunk, C.F., Lee, L.C., Tran, A.B., Li, J., 2003. Complete sequence of the mitochondrial genome of *Tetrahymena thermophila* and comparative methods for identifying highly divergent genes. Nucleic Acids Res. 31, 1673-1682. https://doi.org/10.1093/nar/gkg270.

Burger, G., Zhu, Y., Littlejohn, T.G., Greenwood, S.J., Schnare, M.N., Lang, B.F., Gray, M.W., 2000. Complete sequence of the mitochondrial genome of *Tetrahymena pyriformis* and comparison with *Paramecium aurelia* mitochondrial DNA. J. Mol. Biol. 297, 365-380. https://doi.org/10.1006/jmbi.2000.3529.

Cameron, S.L., Lambkin, C.L., Barker, S.C., Whiting, M.F., 2007. A mitochondrial genome phylogeny of Diptera: whole genome sequence data accurately resolve relationships over broad timescales with high precision. Syst. Entomol. 32, 40-59. https://doi.org/10.1111/j.1365-3113.2006.00355.x.

Cameron, S.L., Lo, N., Bourguignon, T., Svenson, G.J., Evans, T.A., 2012. A mitochondrial genome phylogeny of termites (Blattodea: Termitoidae): Robust support for interfamilial

relationships and molecular synapomorphies define major clades. Mol. Phylogenet. Evol. 65, 163-173. https://doi.org/10.1016/j.ympev.2012.05.034.

Cameron, S.L., Sullivan, J., Song, H., Miller, K.B., Whiting, M.F., 2009. A mitochondrial genome phylogeny of the Neuropterida (lace-wings, alderflies and snakeflies) and their relationship to the other holometabolous insect orders. Zool. Scr. 38, 575-590. https://doi.org/10.1111/j.1463-6409.2009.00392.x.

Carey, P.G., Warren, A., 1983. The role of surface topography in the taxonomy of peritrich ciliates. Protistologica. 19, 73-89.

Chantangsi, C., Lynn, D.H., Brandl, M.T., Cole, J.C., Hetrick, N., Ikonomi, P., 2007. Barcoding ciliates: a comprehensive study of 75 isolates of the genus *Tetrahymena*. Int. J. Syst. Evol. Microbiol. 57, 2412-2425. https://doi.org/10.1099/ijs.0.64865-0.

Clamp, J.C., 1991. Revision of the family Lagenophryidae Bütschli, 1889 and description of the family Usconophryidae n. fam. (Ciliophora, Peritricha). J. Protozool. 38, 355-377. https://doi.org/10.1111/j.1550-7408.1991.tb01373.x.

Clamp, J.C., 2005. Redescription of *Lagenophrys maxillaris* (Jankowski, 1993) (Ciliophora, Peritrichia, Lagenophryidae), an ectosymbiont of marine amphipods. J. Eukaryot. Microbiol. 52, 38-43. https://doi.org/10.1111/j.1550-7408.2005.3302r.x.

Clamp, J.C., 2006. Redescription of *Lagenophrys cochinensis* Santhakumari & Gopalan, 1980 (Ciliophora, Peritrichia, Lagenophryidae), an ectosymbiont of marine isopods, including new information on morphology, geographic distribution, and intraspecific variation. J. Eukaryot. Microbiol. 53, 58-64. https://doi.org/10.1111/j.1550-7408.2005.00074.x.

Corliss, J.O., 1979. The Ciliated Protozoa: Characterization, Classification and Guide to the Literature, 2nd ed. Pergamon, Oxford.

Couch, J.A., 1973. Ultrastructural and protargol studies of *Lagenophrys callinectes* (Ciliophora: Peritrichida). J. Protozool. 20, 638-647. https://doi.org/10.1111/j.1550-7408.1973.tb03588.x.

Coyne, R.S., Hannick, L., Shanmugam, D., Hostetler, J.B., Brami, D., Joardar, V.S., Johnson, J., Radune, D., Singh, I., Badger, J.H., Kumar, U., Saier, M., Wang, Y., Cai, H., Gu, J., Mather, M.W., Vaidya, A.B., Wilkes, D.E., Rajagopalan, V., Asai, D.J., Pearson, C.G., Findly, R.C., Dickerson, H.W., Wu, M., Martens, C., Van de Peer, Y., Roos, D.S., Cassidy-Hanley, D.M., Clark, T.G., 2011. Comparative genomics of the pathogenic ciliate *Ichthyophthirius multifiliis*, its free-living relatives and a host species provide insights into adoption of a parasitic lifestyle and prospects for disease control. Genome Biol. 12, R100. https://doi.org/10.1186/gb-2011-12-10-r100.

da Silva-Neto, I.D., Paiva, T.D.S., Dias, R.J.P., Campos, C.J.A., Migotto, A.E., 2012. Redescription of *Licnophora chattoni* Villeneuve-Brachon, 1939 (Ciliophora, Spirotrichea), associated with *Zyzzyzus warreni* Calder, 1988 (Cnidaria, Hydrozoa). Eur. J. Protistol. 48, 48-62. https://doi.org/10.1016/j.ejop.2011.07.004.

Darriba, D., Taboada, G.L., Doallo, R., Posada, D., 2011. ProtTest 3: fast selection of best-fit models of protein evolution. Bioinformatics. 27, 1164-1165. https://doi.org/10.1093/bioinformatics/btr088.

Darriba, D., Taboada, G.L., Doallo, R., Posada, D., 2012. jModelTest 2: more models, new heuristics and parallel computing. Nat. Methods. 9, 772-772. https://doi.org/10.1038/nmeth.2109.

de Graaf, R.M., Ricard, G., van Alen, T.A., Duarte, I., Dutilh, B.E., Burgtorf, C., Kuiper, J.W.P., van der Staay, G.W.M., Tielens, A.G.M., Huynen, M.A., Hackstein, J.H.P., 2011. The organellar genome and metabolic potential of the hydrogen-producing mitochondrion of *Nyctotherus ovalis*. Mol. Biol. Evol. 28, 2379-2391. https://doi.org/10.1093/molbev/msr059.

de Graaf, R.M., van Alen, T.A., Dutilh, B.E., Kuiper, J.W.P., van Zoggel, H.J.A.A., Huynh, M.B., Görtz, H.-D., Huynen, M.A., Hackstein, J.H.P., 2009. The mitochondrial genomes of the ciliates

Euplotes minuta and *Euplotes crassus*. BMC Genom. 10, 514. https://doi.org/10.1186/1471-2164-10-514.
Dieckmann, J., 1995. An improved protargol impregnation for ciliates yielding reproducible results. Eur. J. Protistol. 31, 372-382. https://doi.org/10.1016/S0932-4739(11)80449-9.
Dubber, D., Gray, N.F., 2011a. The effect of anoxia and anaerobia on ciliate community in biological nutrient removal systems using laboratory-scale sequencing batch reactors (SBRs). Water Res. 45, 2213-2226. https://doi.org/10.1016/j.watres.2011.01.015.
Dubber, D., Gray, N.F., 2011b. The influence of fundamental design parameters on ciliates community structure in Irish activated sludge systems. Eur. J. Protistol. 47, 274-286. https://doi.org/10.1016/j.ejop.2011.05.001.
Dumilag, R.V., Gallardo, W.G.M., Garcia, C.P.C., You, Y., Chaves, A.K.G., Agahan, L., 2018. Phenotypic and mtDNA variation in Philippine *Kappaphycus cottonii* (Gigartinales, Rhodophyta). Mitochondrial DNA A. 29, 951-963. https://doi.org/10.1080/24701394.2017.1398745.
Dunthorn, M., Stoeck, T., Wolf, K., Breiner, H.-W., Foissner, W., 2012. Diversity and endemism of ciliates inhabiting Neotropical phytotelmata. System. Biodivers. 10, 195-205. https://doi.org/10.1080/14772000.2012.685195.
Eperon, S., 1980. Sur la stomatogenèse et les relations phylogenétiques du cilié pèritricha *Thuricola folliculata* (O. F. Müller, 1786). Protistologica. 16, 594-564.
Eperon, S., 1985. Cytokinesis of *Thuricola folliculata* (Ciliophora, Peritrichida). J. Protozool. 32, 296-305. https://doi.org/10.1111/j.1550-7408.1985.tb03054.x.
Eperon, S., Grain, J., 1983. Sur les fibres postciliaires de la polycinétie de *Thuricola folliculata* (O. F. Müller, 1786) (Ciliophora, Peritrichida) en bipartition. Protistologica. 19, 123-130.
Feng, J., Jiang, C., Warren, A., Tian, M., Cheng, J., Liu, G., Xiong, J., Miao, W., 2015. Phylogenomic analyses reveal subclass Scuticociliatia as the sister group of subclass Hymenostomatia within class Oligohymenophorea. Mol. Phylogenet. Evol. 90, 104-111. https://doi.org/10.1016/j.ympev.2015.05.007.
Fenn, J.D., Song, H., Cameron, S.L., Whiting, M.F., 2008. A preliminary mitochondrial genome phylogeny of Orthoptera (Insecta) and approaches to maximizing phylogenetic signal found within mitochondrial genome data. Mol. Phylogenet. Evol. 49, 59-68. https://doi.org/10.1016/j.ympev.2008.07.004.
Ferreira, T., Rasband, W.S., 2012. ImageJ user guide. IJ 1.46r. https://imagej.nih.gov/ij/docs/guide/146.html.
Fish, J.D., Goodwin, B.J., 1976. Observations on the peritrichous ciliate *Scyphidia ubiquita* from the west coast of Wales and a description of a new species. J. Zool. 179, 361-371. https://doi.org/10.1111/j.1469-7998.1976.tb02300.x.
Foissner, W., 1981. Morphologie und Taxonomie einiger heterotricher und peritricher Ciliaten (Protozoa: Ciliophora) aus alpinen Böden. Protistologica. 17, 29-43.
Foissner, W., 1991. Basic light and scanning electron microscopic methods for taxonomic studies of ciliated protozoa. Eur. J. Protistol. 27, 313-330. https://doi.org/10.1016/S0932-4739(11)80248-8.
Foissner, W., 1992a. Estimating the species richness of soil protozoa using the “non-flooded petri dish method”, In: Lee, J.J., Soldo, A.T. (Eds.), Protocols in protozoology. Allen Press, Lawrence, pp. B-10.1-B-10.2.
Foissner, W., 1992b. Protargol methods, In: Lee, J.J., Soldo, A.T. (Eds.), Protocols in Protozoology. Allen Press, Lawrence, pp. C-6.1-C-6.8.
Foissner, W., 2016. Protists as bioindicators in activated sludge: identification, ecology and future needs. Eur. J. Protistol. 55, 75-94. https://doi.org/10.1016/j.ejop.2016.02.004.

Foissner, W., Agatha, S., Berger, H., 2002. Soil ciliates (Protozoa, Ciliophora) from Namibia (Southwest Africa), with emphasis on two contrasting environments, the Etosha region and the Namib Desert. Biologiezentrum des Oberösterreichischen Landesmuseums, Linz.

Foissner, W., Berger, H., Kohmann, F., 1992. Taxonomische und Ökologische Revision der Ciliaten des Saprobiensystems. Band II: Peritrichia, Heterotrichida, Odontostomatida., Informationsberichte des Bayer. Bayerisches Landesamt für Wasserwirtschaft, München.

Foissner, W., Berger, H., Schaumburg, J., 1999. Identification and ecology of limnetic plankton ciliates. Informationsberichte des Bayer. Bayerisches Landesamt für Wasserwirtschaft, München.

Foissner, W., Blake, N., Wolf, K., Breiner, H.-W., Stoeck, T., 2010. Morphological and molecular characterization of some peritrichs (Ciliophora: Peritrichida) from Tank Bromeliads, including two new genera: *Orborhabdostyla* and *Vorticellides*. Acta Protozool. 48, 291-319.

Foissner, W., Schiffmann, H., 1974. Vergleichende studien an argyrophilen strukturen von vierzehn peritrichen ciliaten. Protistologica. 10, 489-508.

Foissner, W., Schiffmann, H., 1975. Biometrische und morphologische untersuchungen über die variabilität von argyrophilen strukturen bei peritrichen Ciliaten. Protistologica. 11, 415-428.

Gao, F., Katz, L.A., Song, W., 2013. Multigene-based analyses on evolutionary phylogeny of two controversial ciliate orders: Pleuronematida and Loxocephalida (Protista, Ciliophora, Oligohymenophorea). Mol. Phylogenet. Evol. 68, 55-63. https://doi.org/10.1016/j.ympev.2013.03.018.

Gao, F., Warren, A., Zhang, Q., Gong, J., Miao, M., Sun, P., Xu, D., Huang, J., Yi, Z., Song, W., 2016. The all-data-based evolutionary hypothesis of ciliated protists with a revised classification of the phylum Ciliophora (Eukaryota, Alveolata). Sci. Rep. 6, 24874. https://doi.org/10.1038/srep24874.

Gao, Y., Jin, S., Dang, H., Ye, S., Li, R., 2018. Mitochondrial genome sequencing of notorious scuticociliates (*Pseudocohnilembus persalinus*) isolated from Turbot (*Scophthalmus maximus* L.). Mitochondrial DNA B. 3, 1077-1078. https://doi.org/10.1080/23802359.2018.1508388.

Gentekaki, E., Kolisko, M., Boscaro, V., Bright, K.J., Dini, F., Di Giuseppe, G., Gong, Y., Miceli, C., Modeo, L., Molestina, R.E., Petroni, G., Pucciarelli, S., Roger, A.J., Strom, S.L., Lynn, D.H., 2014. Large-scale phylogenomic analysis reveals the phylogenetic position of the problematic taxon *Protocruzia* and unravels the deep phylogenetic affinities of the ciliate lineages. Mol. Phylogenet. Evol. 78, 36-42. https://doi.org/10.1016/j.ympev.2014.04.020.

Gentekaki, E., Kolisko, M., Gong, Y., Lynn, D.H., 2017. Phylogenomics solves a long-standing evolutionary puzzle in the ciliate world: The subclass Peritrichia is monophyletic. Mol. Phylogenet. Evol. 106, 1-5. https://doi.org/10.1016/j.ympev.2016.09.016.

Gentekaki, E., Lynn, D.H., 2010. Evidence for cryptic speciation in *Carchesium polypinum* Linnaeus, 1758 (Ciliophora: Peritrichia) inferred from mitochondrial, nuclear, and morphological markers. J. Eukaryot. Microbiol. 57, 508-519. https://doi.org/10.1111/j.1550-7408.2010.00505.x.

Gong, X., 1989a. Descriptions of six new species of peritrich from Xinjiang, China. . Acta Zootaxon. Sin. 14, 396-403.

Gong, X., 1989b. Descriptions of three new species of peritrich from Qinghai province, China. Acta Zootaxon. Sin. 14, 257-260.

González, J., 1978. La structure fine et la reproduction du Cilié Péritriche *Thuricola folliculata* (O.F. Müller, 1786). University of Lausanne, Switzerland.

González, J., 1979. La loge du cilie petriche *Thuricola folliculata* (O. Mueller, 1786): structure, nature chimique et formation. Protistologica. 15, 487-493.

Grant, J.R., Lahr, D.J.G., Rey, F.E., Burleigh, J.G., Gordon, J.I., Knight, R., Molestina, R.E., Katz, L.A., 2012. Gene discovery from a pilot study of the transcriptomes from three diverse

microbial eukaryotes: *Corallomyxa tenera*, *Chilodonella uncinata*, and *Subulatomonas tetraspora*. Protist Genomics. 1, 3-18. https://doi.org/10.2478/prge-2012-0002.
Guindon, S., Gascuel, O., 2003. A simple, fast, and accurate algorithm to estimate large phylogenies by maximum likelihood. Syst. Biol. 52, 696-704. https://doi.org/10.1080/10635150390235520.
Guinea, A., Gil, R., Serrano, S., Sola, A., 1990. Ultrastructural data on the infraciliature of *Astylozoon pyriforme* (Ciliophora: Peritrichida). Trans. Am. Micros. Soc. 109, 247-253. https://doi.org/10.2307/3226795.
Hammann, I., 1952. Ökologische und biologische untersuchungen an süsswasserperitrichen. Arch. Hydrobiol. 47, 177-228.
Hassanin, A., Léger, N., Deutsch, J., 2005. Evidence for multiple reversals of asymmetric mutational constraints during the evolution of the mitochondrial genome of metazoa, and consequences for phylogenetic inferences. Syst. Biol. 54, 277-298. https://doi.org/10.1080/10635150590947843.
ICZN (International Commission on Zoological Nomenclature), 1999. International Code of Zoological Nomenclature. The International Trust for Zoological Nomenclature, London.
Ilyasov, R.A., Poskryakov, A.V., Nikolenko, A.G., 2016. Seven genes of mitochondrial genome enabling differentiation of honeybee subspecies *Apis mellifera*. Russ. J. Genet. 52, 1062-1070. https://doi.org/10.1134/S1022795416090064.
Irwin, N.A.T., Lynn, D.H., 2015. Molecular phylogeny of mobilid and sessilid ciliates symbiotic in estern pacific limpets (Mollusca: Patellogastropoda). J. Eukaryot. Microbiol. 62, 543-552. https://doi.org/10.1111/jeu.12208.
Jiang, C., Wang, G., Xiong, J., Yang, W., Sun, Z., Feng, J., Warren, A., Miao, W., 2019. Insights into the origin and evolution of Peritrichia (Oligohymenophorea, Ciliophora) based on analyses of morphology and phylogenomics. Mol. Phylogenet. Evol. 132, 25-35. https://doi.org/10.1016/j.ympev.2018.11.018.
Küsters, E., 1974. Ökologische und systematische Untersuchungen der Aufwuchsciliaten im Königshafen bei List/Sylt. Arch. Hydrobiol. (Suppl.). 45, 121-211.
Kahl, A., 1935. Urtiere oder Protozoa I: Wimpertiere oder Ciliata (Infusoria) 4. Peritricha und Chonotricha. Tierwelt Dtl. 30, 651-886.
Katoh, K., Standley, D.M., 2013. MAFFT multiple sequence alignment software version 7: improvements in performance and usability. Mol. Biol. Evol. 30, 772-780. https://doi.org/10.1093/molbev/mst010.
Kawamura, R., 1973. The ciliary and fibrillar systems of the ciliate *Vorticella*. J. Sci. Hiroshima Univ. B. 24, 183-203.
Kent, W.S., 1981. A manual of the infusoria: including a description of all known flagellate, ciliate, and tentaculiferous protozoa, British and foreign and an account of the organization and affinities of the sponges. David Bogue, London.
Kher, C.P., Doerder, F.P., Cooper, J., Ikonomi, P., Achilles-Day, U., Küpper, F.C., Lynn, D.H., 2011. Barcoding *Tetrahymena*: discriminating species and identifying unknowns using the cytochrome c oxidase subunit I (cox-1) barcode. Protist. 162, 2-13. https://doi.org/10.1016/j.protis.2010.03.004.
Kishino, H., Miyata, T., Hasegawa, M., 1990. Maximum likelihood inference of protein phylogeny and the origin of chloroplasts. J. Mol. Evol. 31, 151-160. https://doi.org/10.1007/BF02109483.
Konstantynenko, L.A., 2007. The Peritrichia (Ciliophora, Peritrichia) in the activated sludge tank of sewage treatment plant from Zhytomyr. Vestn. Zool. 41, 169-174.
Lasek-Nesselquist, E., Johnson, M.D., 2019. A phylogenomic approach to clarifying the relationship of *Mesodinium* within the Ciliophora: a case study in the complexity of mixed-species transcriptome analyses. Genome Biol. Evol. 11, 3218-3232. https://doi.org/10.1093/gbe/evz233.

Li, L., Song, W., Warren, A., Shin, M.K., Chen, Z., Ji, D., Sun, P., 2008. Reconsideration of the phylogenetic positions of five peritrich genera, *Vorticella*, *Pseudovorticella*, *Zoothamnopsis*, *Zoothamnium*, and *Epicarchesium* (Ciliophora, Peritrichia, Sessilida), based on small subunit rRNA gene sequences. J. Eukaryot. Microbiol. 55, 448-456. https://doi.org/10.1111/j.1550-7408.2008.00351.x.

Li, L., Song, W., Warren, A., Wang, Y., Ma, H., Hu, X., Chen, Z., 2006. Phylogenetic position of the marine ciliate, *Cardiostomatella vermiforme* (Kahl, 1928) Corliss, 1960 inferred from the complete SSrRNA gene sequence, with establishment of a new order Loxocephalida n. ord. (Ciliophora, Oligohymenophorea). Eur. J. Protistol. 42, 107-114. https://doi.org/10.1016/j.ejop.2006.01.004.

Li, R., Gao, Y., Hou, Y., Ye, S., Wang, L., Sun, J., Li, Q., 2018. Mitochondrial genome sequencing and analysis of scuticociliates (*Uronema marinum*) isolated from Takifugu rubripes. Mitochondrial DNA B. 3, 736-737. https://doi.org/10.1080/23802359.2018.1483757.

Liang, Z., Shen, Z., Zhang, Y., Ji, D., Li, J., Warren, A., Lin, X., 2019. Morphology and phylogeny of four new *Vorticella* Species (Ciliophora: Peritrichia) from coastal waters of southern China. J. Eukaryot. Microbiol. 66, 267-280. https://doi.org/10.1111/jeu.12668.

Lom, J., 1964. The morphology and morphogenesis of the buccal ciliary organelles in some peritrichous ciliates. Arch. Protistenk. 107, 131-162.

Lom, J., Corliss, J.O., 1968. Observations on the fine structure of two species of the peritrich ciliate genus *Scyphidia* and on their mode of attachment to their host. Trans. Am. Micros. Soc. 87, 493-509. https://doi.org/10.2307/3224224.

Lu, B., Ji, D., Sheng, Y., Song, W., Hu, X., Chen, X., Al-Rasheid, K.A.S., 2018. New discoveries of the genus *Thuricola* Kent, 1881 (Ciliophora, Peritrichia, Vaginicolidae), with descriptions of three poorly known species from China. Acta Protozool. 57, 123-143. https://doi.org/10.4467/16890027ap.18.011.8985.

Lu, B., Li, L., Hu, X., Ji, D., Al-Rasheid, K.A.S., Song, W., 2019. Novel contributions to the peritrich family Vaginicolidae (Protista: Ciliophora), with morphological and phylogenetic analyses of poorly known species of *Pyxicola*, *Cothurnia* and *Vaginicola*. Zool. J. Linn. Soc. 187, 1-30. https://doi.org/10.1093/zoolinnean/zlz009.

Lu, B., Shen, Z., Zhang, Q., Hu, X., Warren, A., Song, W., 2020. Morphology and molecular analyses of four epibiotic peritrichs on crustacean and polychaete hosts, including descriptions of two new species (Ciliophora, Peritrichia). Eur. J. Protistol. 73. https://doi.org/10.1016/j.ejop.2019.125670.

Lynn, D.H., 2008. The Ciliated Protozoa: Characterization, Classification, and Guide to the Literature, 3rd ed. Springer, Dordrecht.

Lynn, D.H., Kolisko, M., 2017. Molecules illuminate morphology: phylogenomics confirms convergent evolution among 'oligotrichous' ciliates. Int. J. Syst. Evol. Microbiol. 67, 3676-3682. https://doi.org/10.1099/ijsem.0.002060.

Lynn, D.H., Kolisko, M., Bourland, W., 2018. Phylogenomic analysis of *Nassula variabilis* n. sp., *Furgasonia blochmanni*, and *Pseudomicrothorax dubius* confirms a nassophorean clade. Protist. 169, 180-189. https://doi.org/10.1016/j.protis.2018.02.002.

Lynn, D.H., Small, E.B., 2002. Phylum Ciliophora, Doflein, 1901., In: Lee, J.J., Leedale, G.F., Bradbury, P.C. (Eds.), An Illustrated Guide to the Protozoa. Allen Press, Lawrence.

Madoni, P., 2011. Protozoa in wastewater treatment processes: a minireview. Ital. J. Zool. 78, 3-11. https://doi.org/10.1080/11250000903373797.

Martin-Cereceda, M., Guinea, A., Bonaccorso, E., Dyal, P., Novarino, G., Foissner, W., 2007. Classification of the peritrich ciliate *Opisthonecta matiensis* (Martin-Cereceda et al. 1999) as *Telotrochidium matiense* nov comb., based on new observations and SSU rDNA phylogeny. Eur. J. Protistol. 43, 265-279. https://doi.org/10.1016/j.ejop.2007.04.003.

Matsunaga, K., Kubota, K., Harada, H., 2014. Molecular diversity of eukaryotes in municipal wastewater treatment processes as revealed by 18S rRNA gene analysis. Microbes Environ. 29, 401-407. https://doi.org/10.1264/jsme2.ME14112.

McKanna, J.A., 1973. Cyclic membrane flow in the ingestive-digestive system of peritrich protozoans. J. Cell. Sci. 13, 663-675.

Medlin, L., Elwood, H.J., Stickel, S., Sogin, M.L., 1988. The characterization of enzymatically amplified eukaryotic 16S-like rRNA-coding regions. Gene. 71, 491-499. https://doi.org/10.1016/0378-1119(88)90066-2.

Miao, W., Fen, W., Yu, Y., Zhang, X., Shen, Y., 2004. Phylogenetic relationships of the Subclass Peritrichia (Oligohymenophorea, Ciliophora) inferred from small subunit rRNA gene sequences. J. Eukaryot. Microbiol. 51, 180-186. https://doi.org/10.1111/j.1550-7408.2004.tb00543.x.

Miao, W., Yu, Y., Shen, Y., 2001. Phylogenetic relationships of the subclass Peritrichia (Oligohymenophorea, Ciliophora) with emphasis on the genus *Epistylis*, inferred from small subunit rRNA gene sequences. J. Eukaryot. Microbiol. 48, 583-587. https://doi.org/10.1111/j.1550-7408.2001.tb00194.x.

Moradian, M.M., Beglaryan, D., Skozylas, J.M., Kerikorian, V., 2007. Complete mitochondrial genome sequence of three *Tetrahymena* species reveals mutation hot spots and accelerated nonsynonymous substitutions in Ymf genes. Plos One. 2, e650. https://doi.org/10.1371/journal.pone.0000650.

Munir, S., Sun, J., 2018. The first snapshot study on horizontal distribution and identification of five peritrich ciliates (Genus *Vorticella* Linnaeus and *Zoothamnium* Bory de St. Vincent) from the eastern Indian Ocean. Acta Oceanol. Sin. 37, 79-85. https://doi.org/10.1007/s13131-018-1303-4.

Nguyen, L.-T., Schmidt, H.A., von Haeseler, A., Minh, B.Q., 2015. IQ-TREE: a fast and effective stochastic algorithm for estimating maximum-likelihood phylogenies. Mol. Biol. Evol. 32, 268-274. https://doi.org/10.1093/molbev/msu300.

Nicolau, A., Dias, N., Mota, M., Lima, N., 2001. Trends in the use of protozoa in the assessment of wastewater treatment. Res. Microbiol. 152, 621-630. https://doi.org/10.1016/S0923-2508(01)01241-4.

Nitla, V., Serra, V., Fokin, S.I., Modeo, L., Verni, F., Sandeep, B.V., Kalavati, C., Petroni, G., 2019. Critical revision of the family Plagiopylidae (Ciliophora: Plagiopylea), including the description of two novel species, *Plagiopyla ramani* and *Plagiopyla narasimhamurtii*, and redescription of *Plagiopyla nasuta* Stein, 1860 from India. Zool. J. Linn. Soc. 186, 1-45. https://doi.org/10.1093/zoolinnean/zly041.

Nusch, E.A., 1970. Ökologische und systematische Untersuchungen der Peritricha (Protozoa, Ciliata) im Aufwuchs von Talsperren und Flusstauen mit verschiedenem Saprobitatsgrad (mit Modellversuchen). Arch. Hydrobiol. (Suppl.). 37, 243-386.

Pan, B., Chen, X., Hou, L., Zhang, Q., Qu, Z., Warren, A., Miao, M., 2019. Comparative genomics analysis of ciliates provides insights on the evolutionary history within "Nassophorea-Synhymenia-Phyllopharyngea" assemblage. Front. Microbiol. 10. https://doi.org/10.3389/fmicb.2019.02819.

Pan, X., Bourland, W.A., Song, W., 2013. Protargol synthesis: an in-house protocol. J. Eukaryot. Microbiol. 60, 609-614. https://doi.org/10.1111/jeu.12067.

Park, K.M., Min, G.S., Kim, S., 2019a. The mitochondrial genome of the ciliate *Pseudourostyla cristata* (Ciliophora, Urostylida). Mitochondrial DNA B. 4, 66-67. https://doi.org/10.1080/23802359.2018.1536458.

Park, M.H., Jung, J.H., Jo, E., Park, K.M., Baek, Y.S., Kim, S.J., Min, G.S., 2019b. Utility of mitochondrial *CO1* sequences for species discrimination of Spirotrichea ciliates (Protozoa,

Ciliophora). Mitochondrial DNA A. 30, 148-155. https://doi.org/10.1080/24701394.2018.1464563.
Pritchard, A.E., Seilhamer, J.J., Mahalingam, R., Sable, C.L., Venuti, S.E., Cummings, D.J., 1990. Nucleotide sequence of the mitochondrial genome of *Paramecium*. Nucleic Acids Res. 18, 173-180. https://doi.org/10.1093/nar/18.1.173.
Quast, C., Pruesse, E., Yilmaz, P., Gerken, J., Schweer, T., Yarza, P., Peplies, J., Glöckner, F.O., 2012. The SILVA ribosomal RNA gene database project: improved data processing and web-based tools. Nucleic Acids Res. 41, D590-D596. https://doi.org/10.1093/nar/gks1219.
Ronquist, F., Teslenko, M., van der Mark, P., Ayres, D.L., Darling, A., Höhna, S., Larget, B., Liu, L., Suchard, M.A., Huelsenbeck, J.P., 2012. MrBayes 3.2: efficient bayesian phylogenetic inference and model choice across a large model space. Syst. Biol. 61, 539-542. https://doi.org/10.1093/sysbio/sys029.
Rosenberg, L.E., Grim, J.N., 1966. Ultrastructure of some buccal organelles of *Opisthonecta*. J. Microsc. (Paris). 5, 787-790.
Ruiz, M.S., Anadon, R., 1988. The cortex and associated structures of the peritrich ciliate *Opercularia coarctata* Claparede and Lachmann. a light and electron microscopical study. Arch. Protistenk. 136, 249-261. https://doi.org/10.1016/S0003-9365(88)80024-1.
Schnare, M.N., Heinonen, T.Y., Young, P.G., Gray, M.W., 1986. A discontinuous small subunit ribosomal RNA in *Tetrahymena pyriformis* mitochondria. J. Biol. Chem. 261, 5187-5193.
Seemann, T., 2014. Prokka: rapid prokaryotic genome annotation. Bioinformatics. 30, 2068-2069. https://doi.org/10.1093/bioinformatics/btu153.
Serra, V., Gammuto, L., Nitla, V., Castelli, M., Lanzoni, O., Sassera, D., Bandi, C., Sandeep, B.V., Verni, F., Modeo, L., Petroni, G., 2020. Morphology, ultrastructure, genomics, and phylogeny of *Euplotes vanleeuwenhoeki* sp. nov. and its ultra-reduced endosymbiont "*Candidatus* Pinguicoccus supinus" sp. nov. Sci. Rep., in press.
Serrano, S., Arregui, L., Perez-Uz, B., Calvo, P., Guinea, A., 2008. Guidelines for the identification of ciliates in wastewater treatment plants, 1st ed. IWA Publishing, London.
Shen, Y., Gu, M., 2016. Fauna Sinica: Invertebrata vol. 45 Ciliophora Oligohymenophorea Peritrichida. Science Press, Beijing.
Sheng, Y., He, M., Zhao, F., Shao, C., Miao, M., 2018. Phylogenetic relationship analyses of complicated class Spirotrichea based on transcriptomes from three diverse microbial eukaryotes: *Uroleptopsis citrina*, *Euplotes vannus* and *Protocruzia tuzeti*. Mol. Phylogenet. Evol. 129, 338-345. https://doi.org/10.1016/j.ympev.2018.06.025.
Sommer, G., 1951. Die peritrichen Ciliaten des Grossen Plöner Sees. Arch. Hydrobiol. 44, 349-440.
Stamatakis, A., 2014. RAxML version 8: a tool for phylogenetic analysis and post-analysis of large phylogenies. Bioinformatics. 30, 1312-1313. https://doi.org/10.1093/bioinformatics/btu033.
Stiller, J., 1971. Szájkoszorús csillósok. - Peritricha. Fauna Hung. 105, 1-245.
Strüder-Kypke, M.C., Lynn, D.H., 2010. Comparative analysis of the mitochondrial cytochrome c oxidase subunit I (COI) gene in ciliates (Alveolata, Ciliophora) and evaluation of its suitability as a biodiversity marker. System. Biodivers. 8, 131-148. https://doi.org/10.1080/14772000903507744.
Strüder-Kypke, M.C., Wright, A.D.G., Fokin, S.I., Lynn, D.H., 2000. Phylogenetic relationships of the genus *Paramecium* inferred from small subunit rRNA gene sequences. Mol. Phylogenet. Evol. 14, 122-130. https://doi.org/10.1006/mpev.1999.0686.
Sun, P., Al-Farraj, S.A., Warren, A., Ma, H., 2017a. Morphology of four new solitary sessile peritrich ciliates from the Yellow Sea, China, with description of an unidentified species of *Paravorticella* (Ciliophora, Peritrichia). Eur. J. Protistol. 57, 73-84. https://doi.org/10.1016/j.ejop.2016.11.001.

Sun, P., Clamp, J., Xu, D., Huang, B., Shin, M.K., 2016. An integrative approach to phylogeny reveals patterns of environmental distribution and novel evolutionary relationships in a major group of ciliates. Sci. Rep. 6, 21695. https://doi.org/10.1038/srep21695.

Sun, P., Ji, D., Warren, A., Song, W., 2009. Solitary sessilid peritrichs, In: Song, W., Warren, A., Hu, X. (Eds.), Free-living ciliates in the Bohai and Yellow Seas, China. Science Press, Beijing, pp. 251-254.

Sun, Z., Jiang, C., Feng, J., Yang, W., Li, M., Miao, W., 2017b. Phylogenomic analysis of *Balantidium ctenopharyngodoni* (Ciliophora, Litostomatea) based on single-cell transcriptome sequencing. Parasite. 24, 43. https://doi.org/10.1051/parasite/2017043.

Suyama, Y., Miura, K., 1968. Size and structural variations of mitochondrial DNA. Proc. Natl. Acad. Sci. U.S.A. 60, 235-242. https://doi.org/10.1073/pnas.60.1.235.

Swart, E.C., Nowacki, M., Shum, J., Stiles, H., Higgins, B.P., Doak, T.G., Schotanus, K., Magrini, V.J., Minx, P., Mardis, E.R., Landweber, L.F., 2012. The *Oxytricha trifallax* mitochondrial genome. Genome Biol. Evol. 4, 136-154. https://doi.org/10.1093/gbe/evr136.

Trueba, F.J., 1978. A taxonomic revision of the peritrich ciliate genus *Pyxicola*. Beaufortia. 27, 219-243.

Trueba, F.J., 1980. A taxonomic revision of the peritrich ciliate genera *Thuricola* and *Pseudothuricola*. Beaufortia. 30, 125-138.

Utz, L.R.P., Eizirik, E., 2007. Molecular phylogenetics of Subclass Peritrichia (Ciliophora : Oligohymenophorea) based on expanded analyses of 18S rRNA sequences. J. Eukaryot. Microbiol. 54, 303-305. https://doi.org/10.1111/j.1550-7408.2007.00260.x.

Utz, L.R.P., Simão, T.L.L., Safi, L.S.L., Eizirik, E., 2010. Expanded phylogenetic representation of genera *Opercularia* and *Epistylis* sheds light on the evolution and higher-level taxonomy of peritrich ciliates (Ciliophora: Peritrichia). J. Eukaryot. Microbiol. 57, 415-420. https://doi.org/10.1111/j.1550-7408.2010.00497.x.

Wang, C., Yan, Y., Chen, X., Al-Farraj, S.A., El-Serehy, H.A., Gao, F., 2019. Further analyses on the evolutionary "key-protist" *Halteria* (Protista, Ciliophora) based on transcriptomic data. Zool. Scr. 48, 813-825. https://doi.org/10.1111/zsc.12380.

Warren, A., 1983. The ecology, morphology and taxonomy of freshwater peritrich ciliates. University of Surrey, England.

Warren, A., Paynter, J., 1991. A revision of *Cothurnia* (Ciliophora: Peritrichida) and its morphological relatives. Bull. Br. Mus. Nat. Hist. Zool. 57, 17-59.

Westram, R., Bader, K., Prüsse, E., Kumar, Y., Meier, H., Glöckner, F.O., Ludwig, W., 2011. ARB: A Software Environment for Sequence Data, In: de Bruijn, F.J. (Ed.), Handbook of Molecular Microbial Ecology I: Metagenomics and Complementary Approaches. Wiley-Blackwell, United States, pp. 399-406.

Wilbert, N., 1975. Eine verbesserte Technik der Protargolimprägnation für Ciliaten. Mikrokosmos. 64, 171-179.

Wu, T., Li, Y., Lu, B., Shen, Z., Song, W., Warren, A., 2020. Morphology, taxonomy and molecular phylogeny of three marine peritrich ciliates, including two new species: *Zoothamnium apoarbuscula* n. sp. and *Z. apohentscheli* n. sp. (Protozoa, Ciliophora, Peritrichia). Mar. Life Sci. Technol. https://doi.org/10.1007/s42995-020-00046-y.

Xu, K., Lei, Y., Al-Rasheid, K.A.S., Song, W., 2011. Two new ectoparasitic ciliates, *Sphenophrya solinis* sp. nov. and *Planeticovorticella paradoxa* sp. nov. (Protozoa: Ciliophora), from marine molluscs. J. Mar. Biolog. Assoc. U.K. 91, 265-274. https://doi.org/10.1017/S0025315410001967.

Xu, Z., 1990. Notes on two new species of genus *Thuricola* from Tianjin. Acta Zootaxon. Sin. 15, 6-9.

Zhao, Y., Gentekaki, E., Yi, Z., Lin, X., 2013. Genetic differentiation of the mitochondrial cytochrome oxidase c subunit I gene in genus *Paramecium* (Protista, Ciliophora). Plos One. 8, e77044. https://doi.org/10.1371/journal.pone.0077044.

Zhou, T., Wang, Z., Yang, H., Gu, Z., 2019. Two new colonial peritrich ciliates (Ciliophora, Peritrichia, Sessilida) from China: With a note on taxonomic distinction between Epistylididae and Operculariidae. Eur. J. Protistol. 70, 17-31. https://doi.org/10.1016/j.ejop.2019.05.003.

Zhuang, Y., Clamp, J.C., Yi, Z., Ji, D., 2016. A new peritrich ciliate from a hypersaline habitat in Northern China. Zootaxa. 4169, 179-186. https://doi.org/10.11646/zootaxa.4169.1.10.

Figure 1

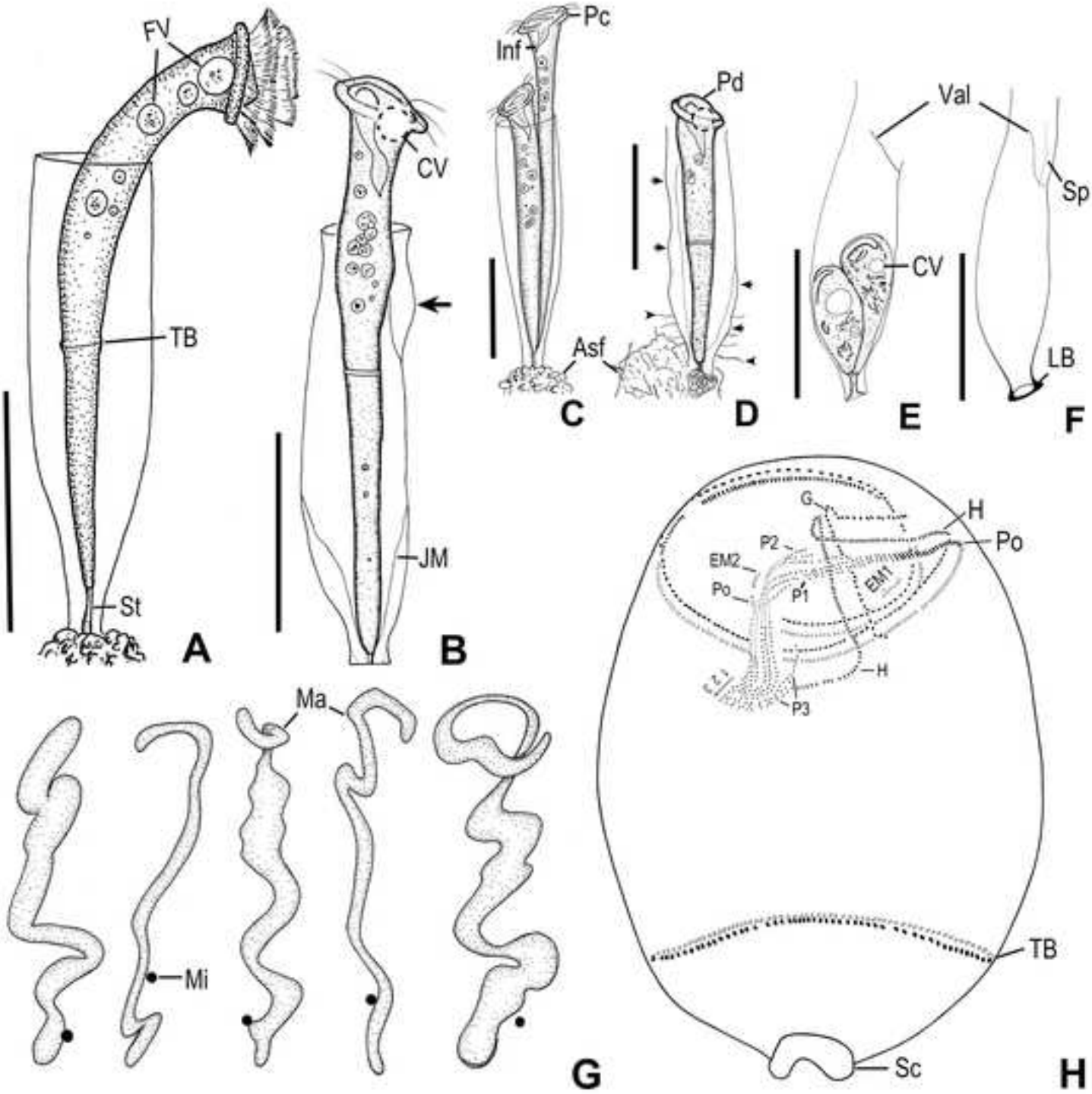

Figure 2

Click here to access/download;Figure;Fig.2.tif

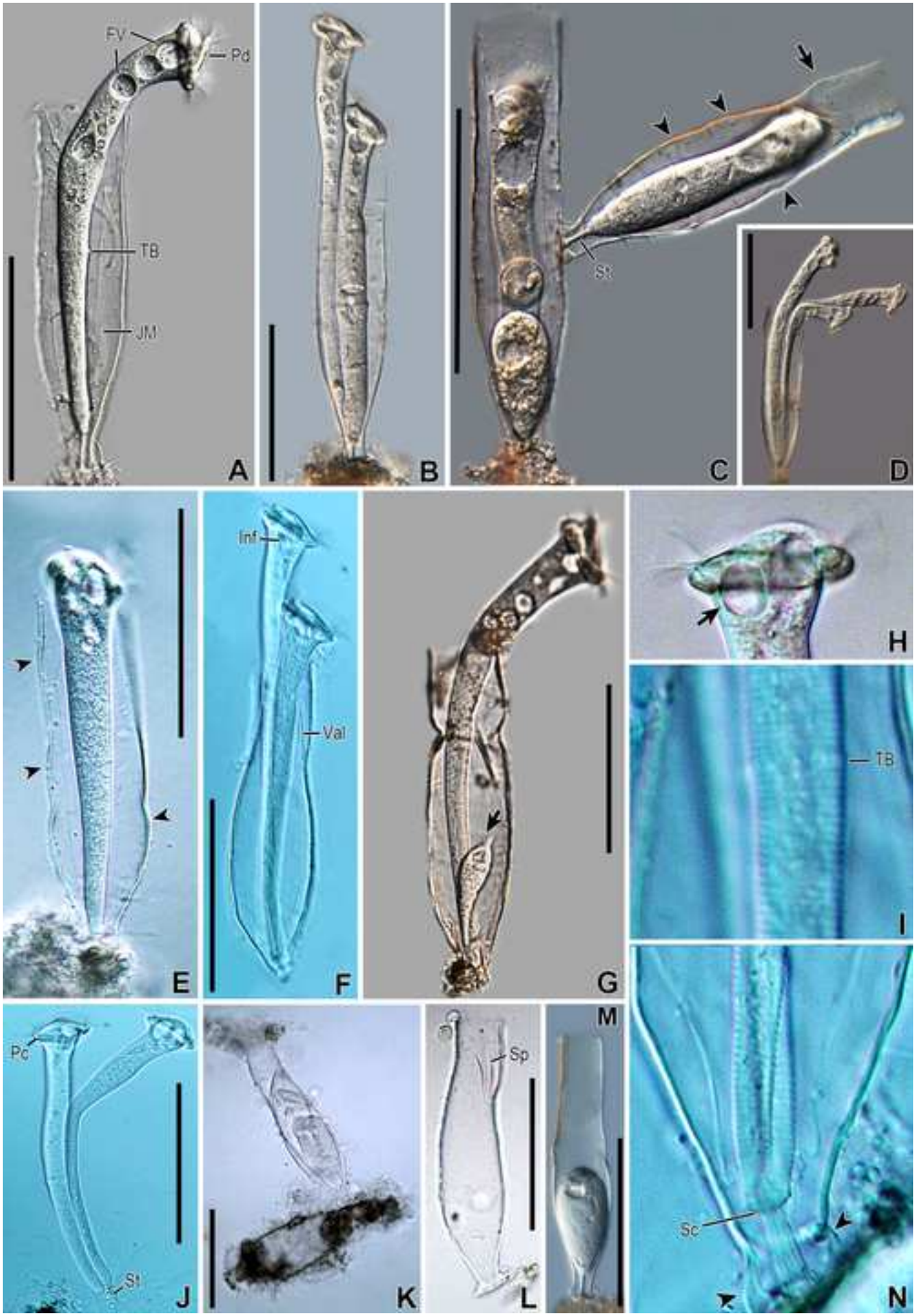

Figure 3

Click here to access/download;Figure;Fig.3.tif

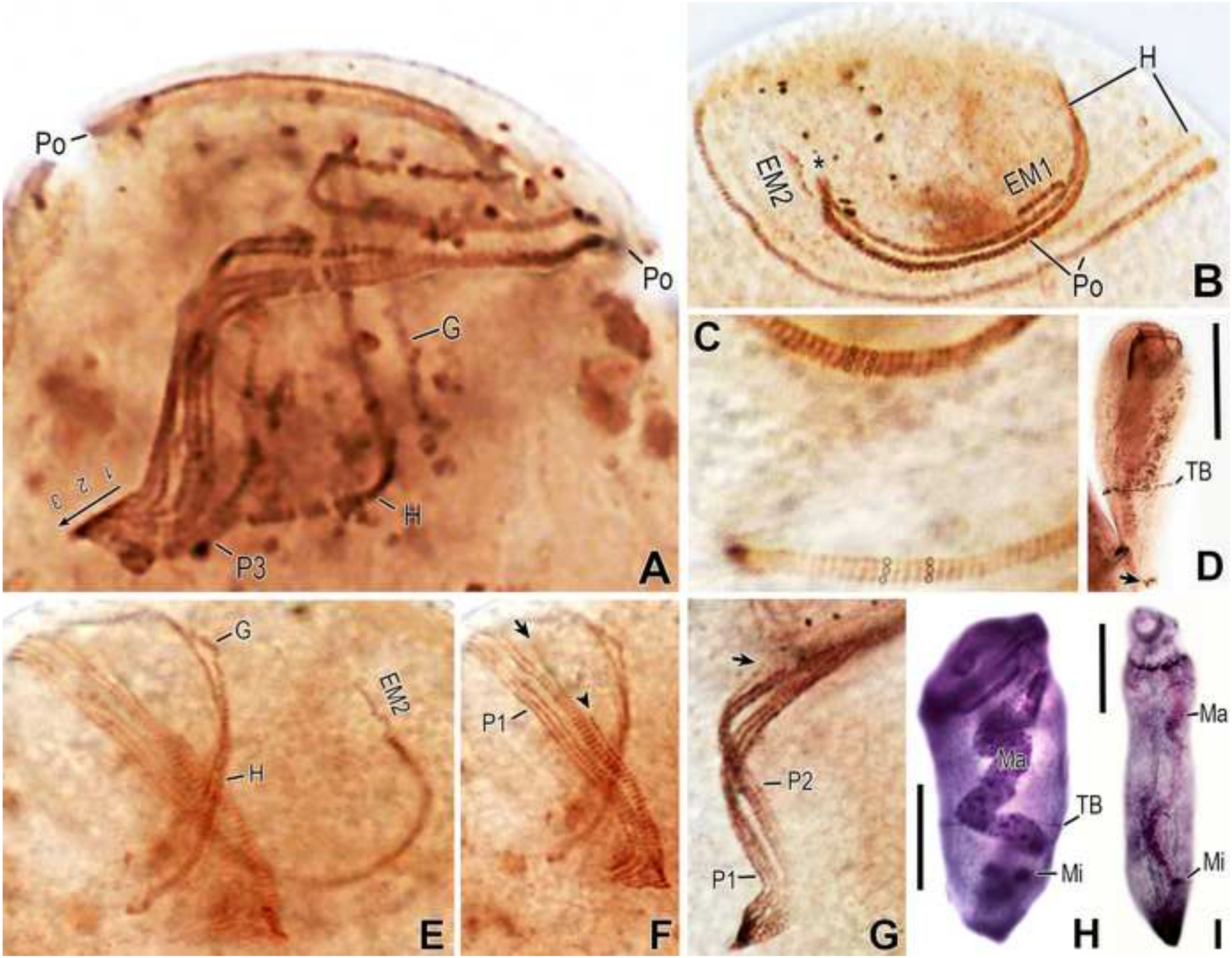

Figure 4

Click here to access/download;Figure;Fig. 4.tif

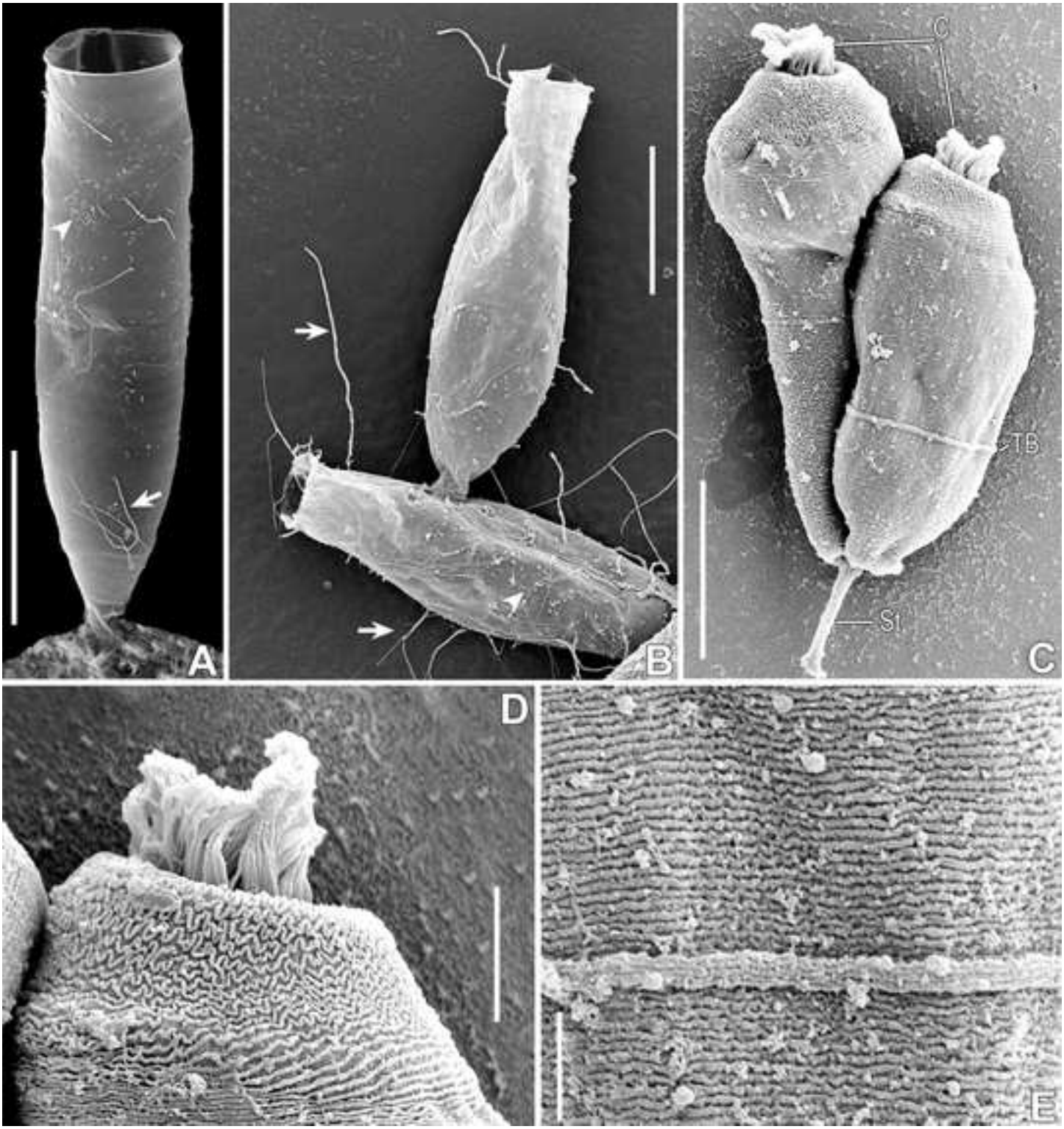

Figure 5

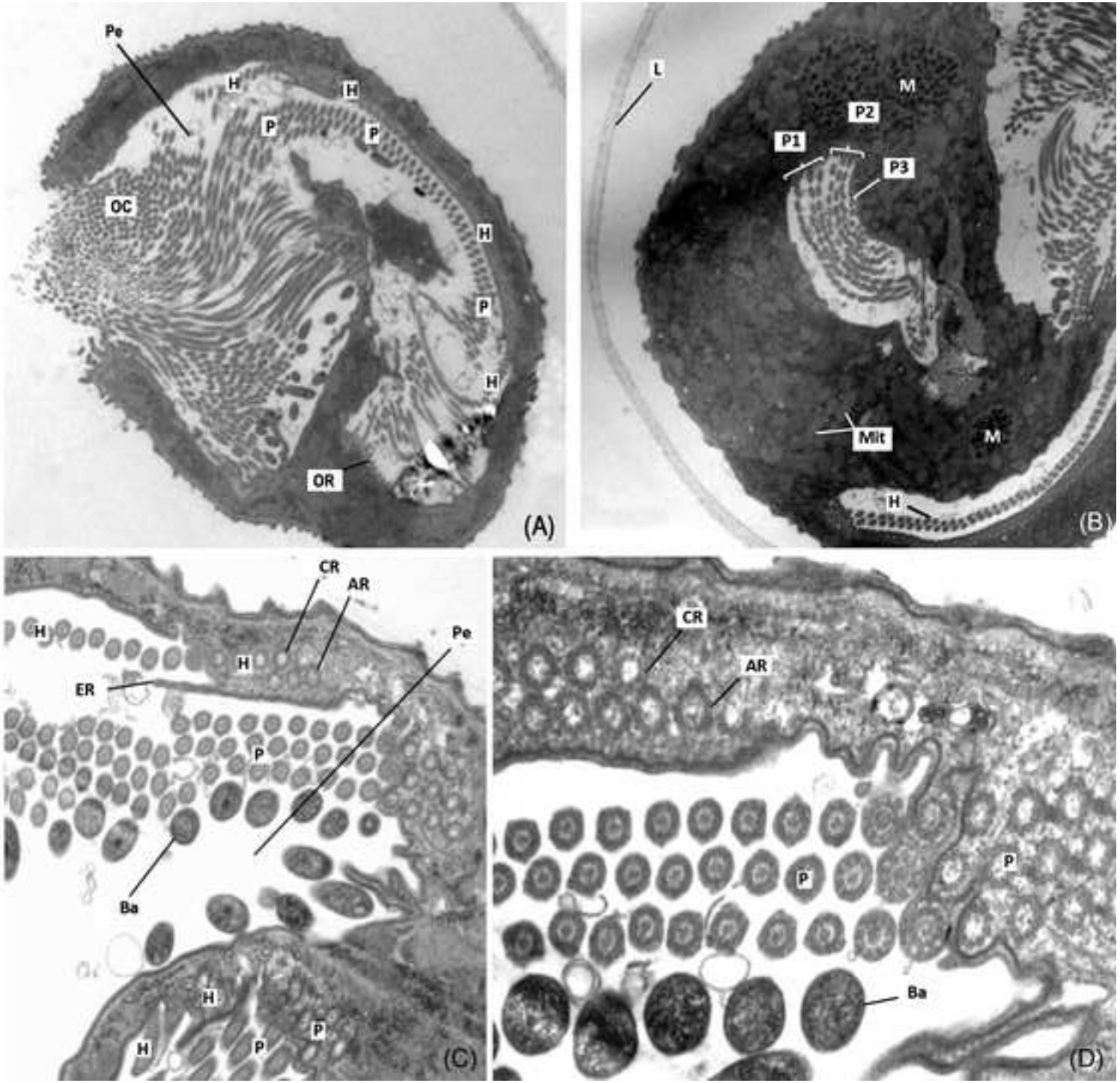

Figure 6

Click here to access/download;Figure;Fig_6_V_PEDRO_final.tif

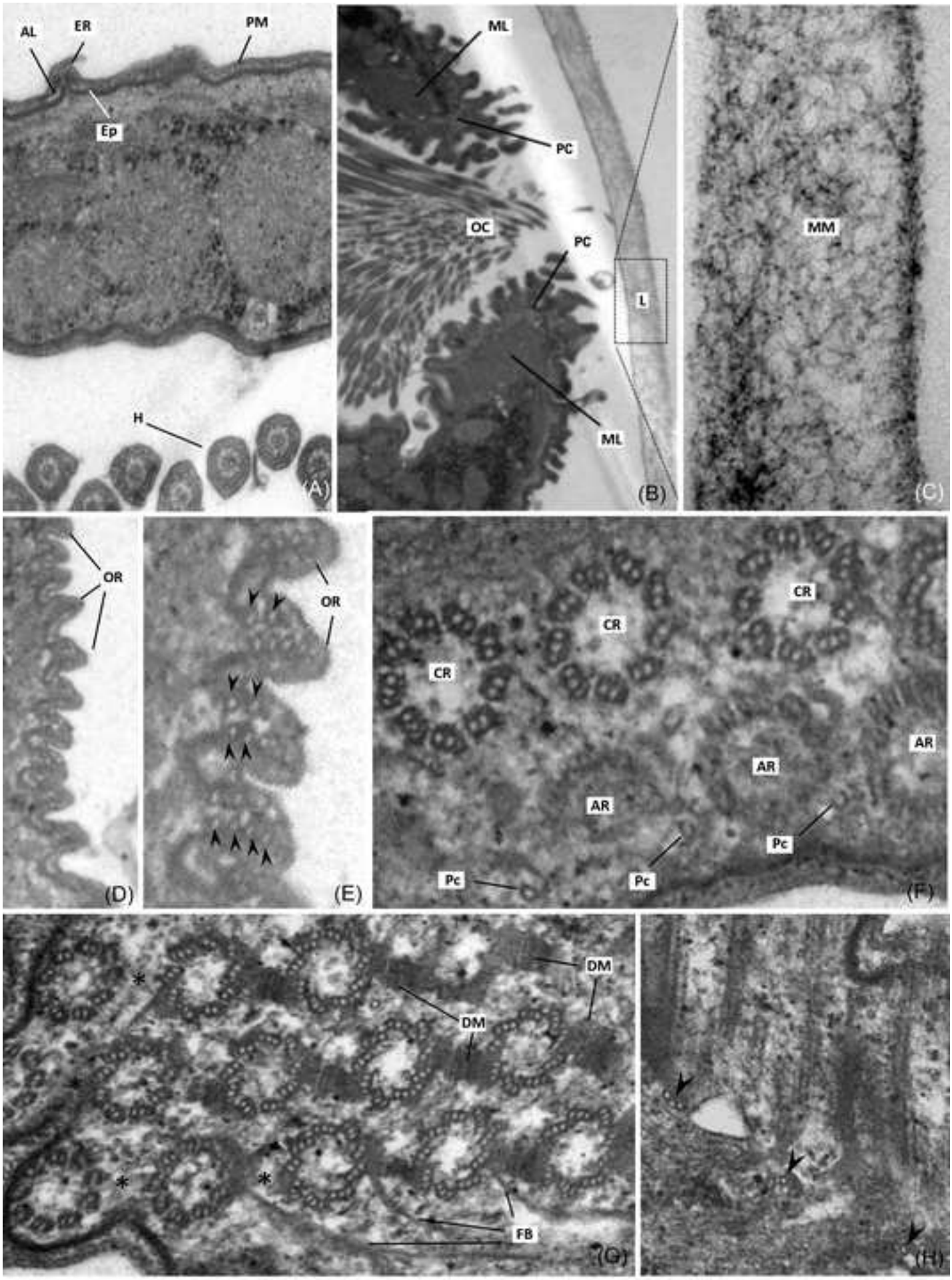

Figure 7

Click here to access/download;Figure;Fig_7_V_PEDRO_final.tif

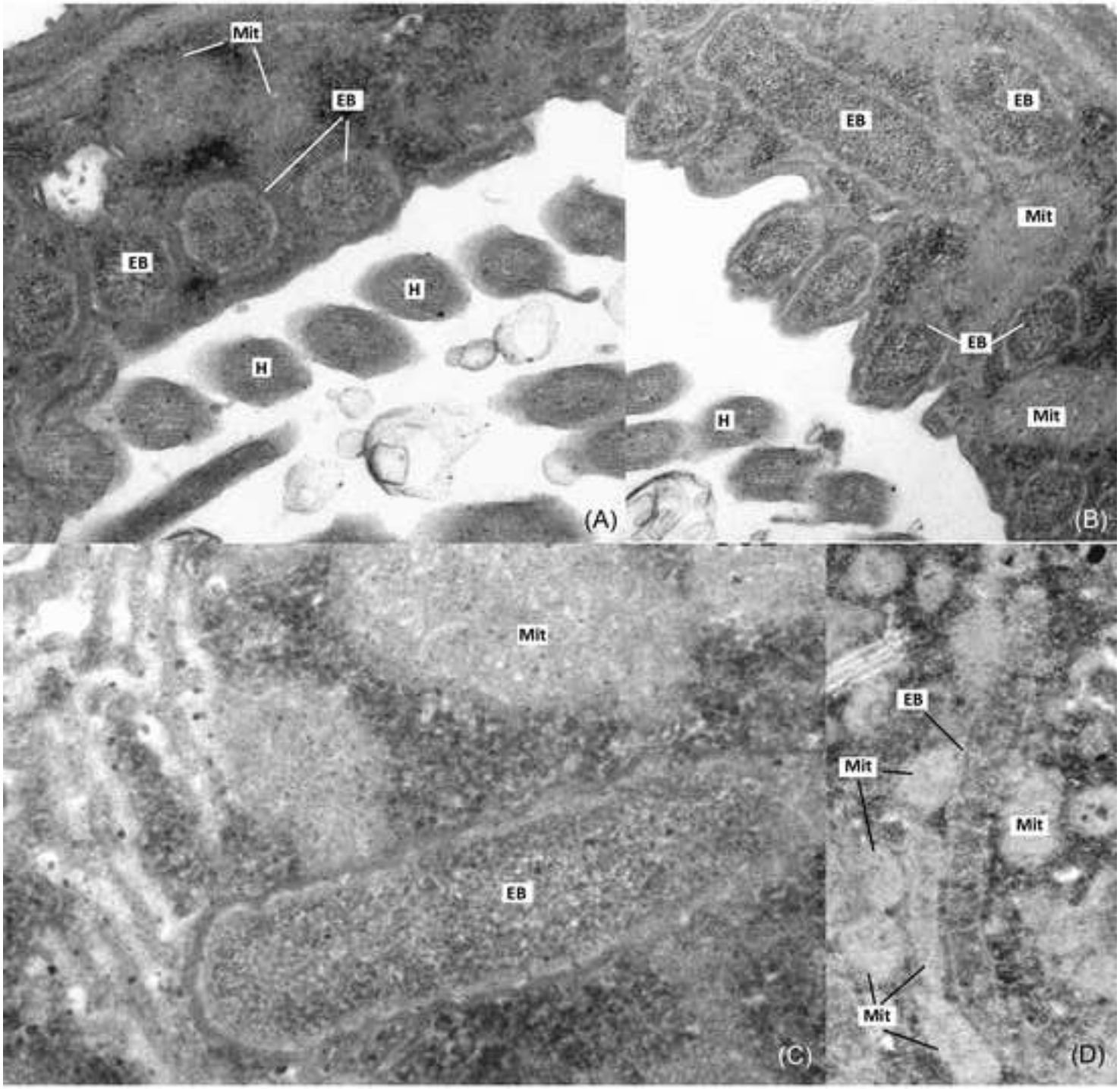

Figure 8

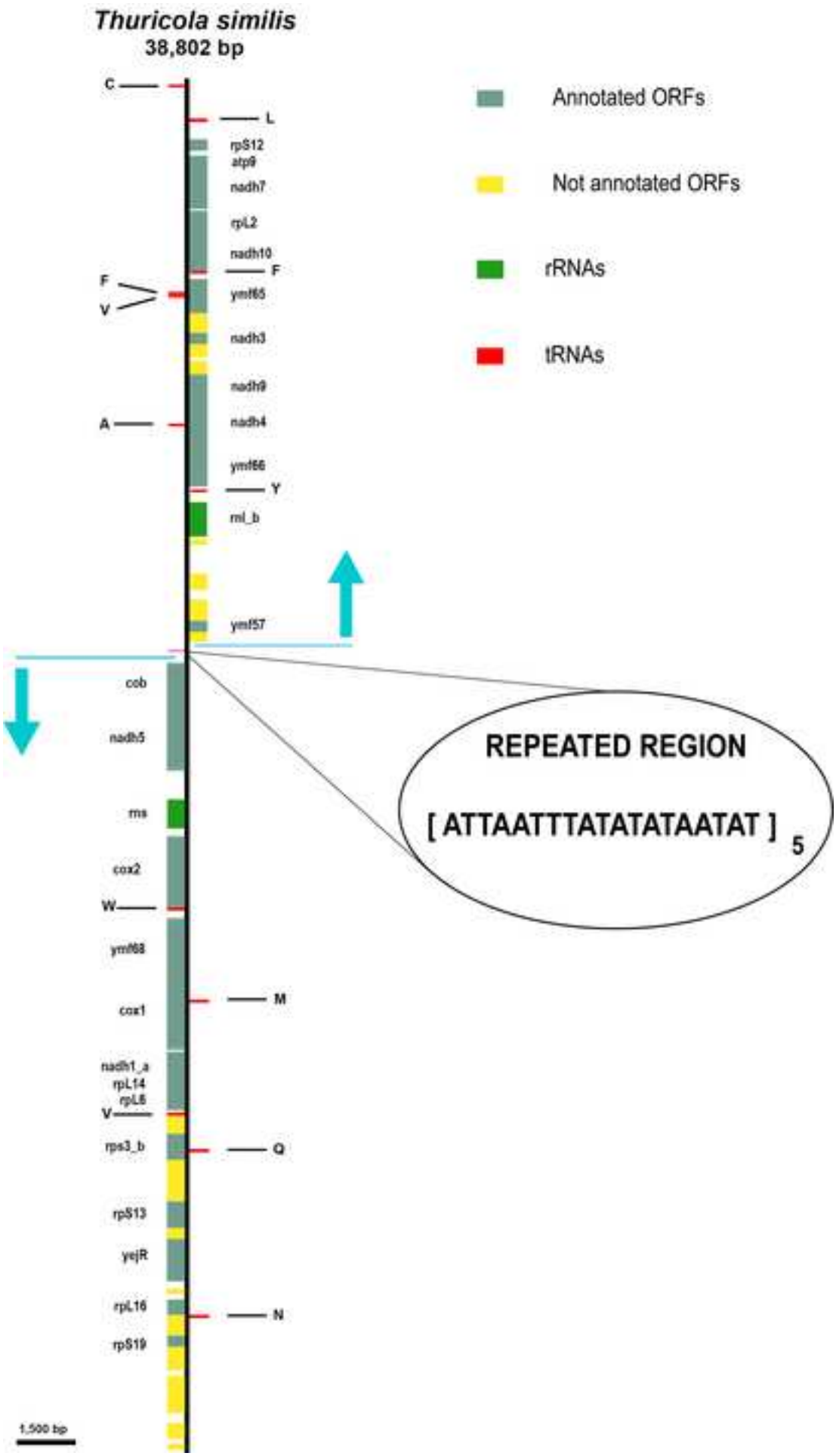

Figure 9

Click here to access/download;Figure;FIG.9.tif

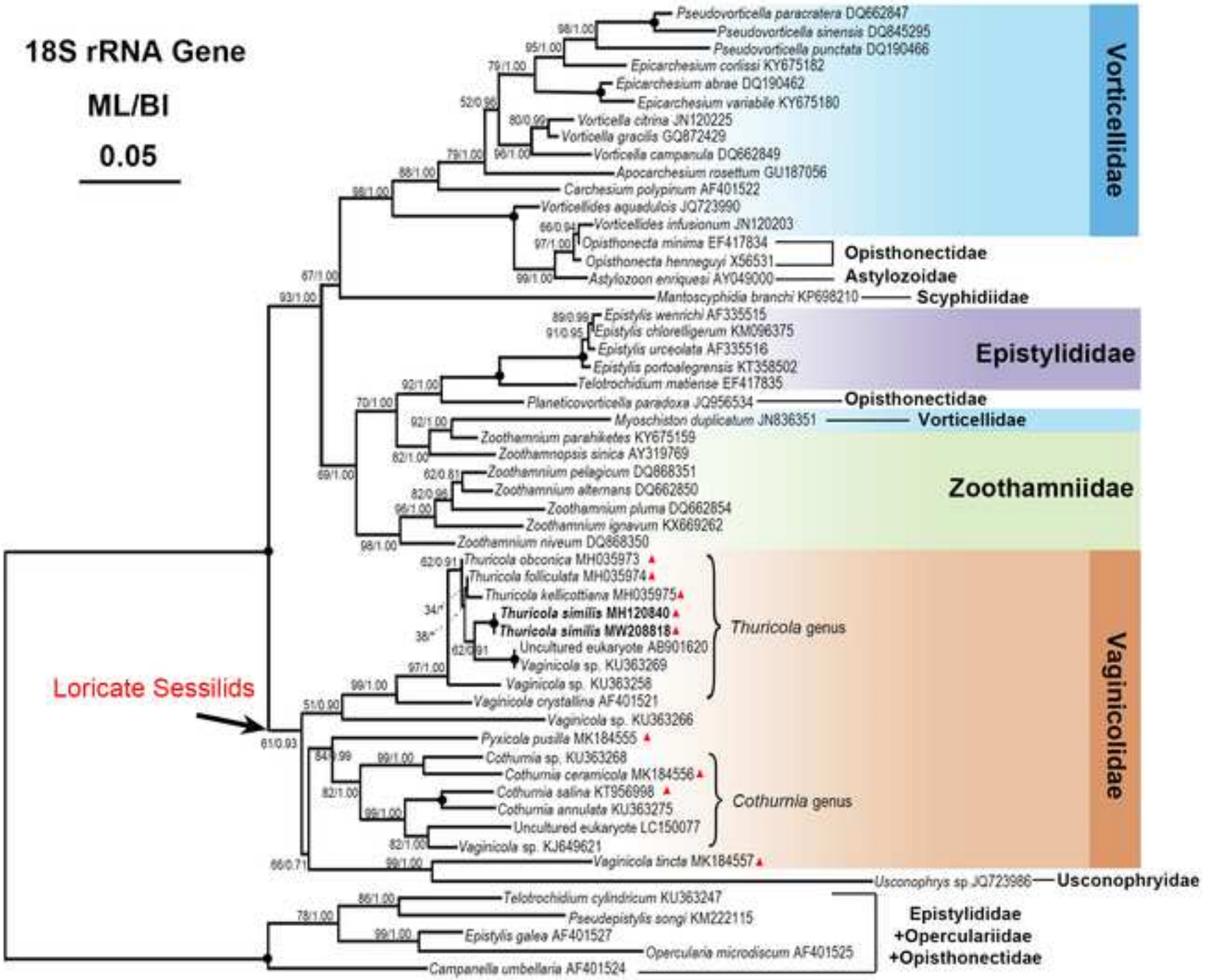

Figure 10

Click here to access/download;Figure;Fig. 10.tif

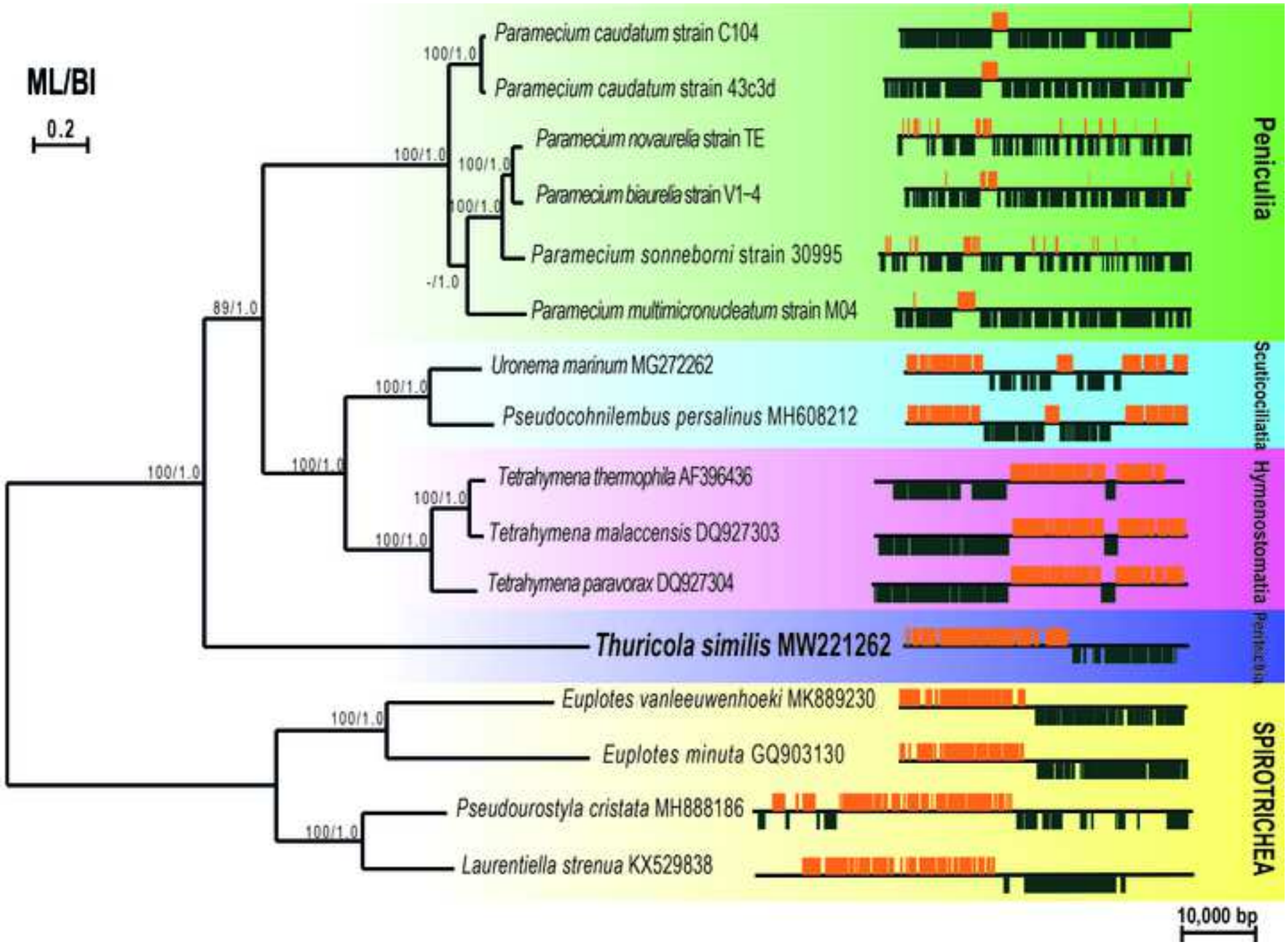

Figure 11

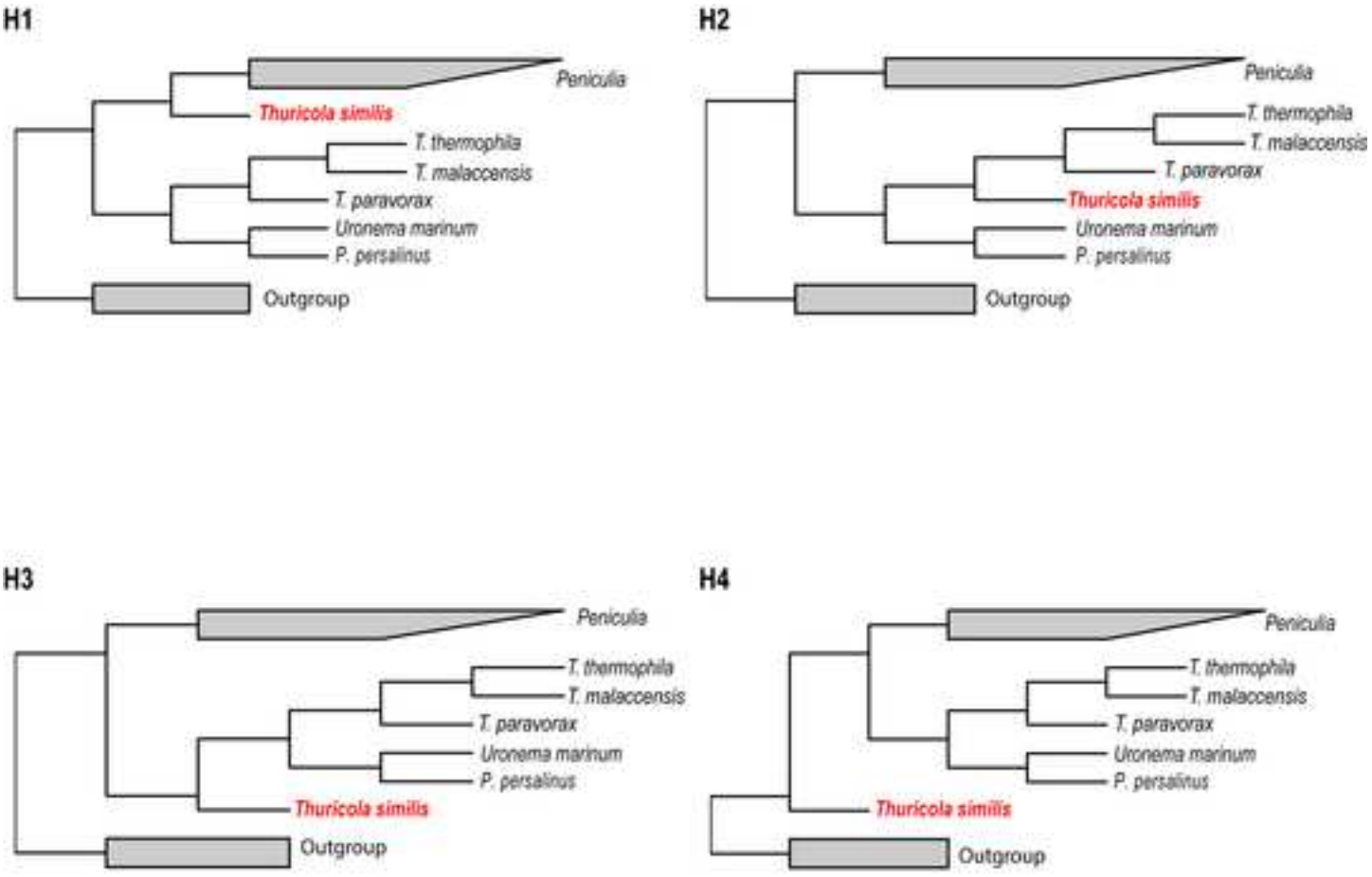

Tree	logL	deltaL	bp-RELL	p-KH	p-SH	p-WKH	p-WSH	c-ELW	p-AU
H1	-114018.09	7.25	**0.202 +**	**0.217 +**	**0.496 +**	**0.217 +**	**0.429 +**	**0.205 +**	**0.27 +**
H2	-114118.00	107.16	0 -	0 -	0 -	0 -	0 -	7.14e-24 -	6.05e-53 -
H3	-114023.29	12.449	0.0284 -	**0.0594 +**	**0.316 +**	**0.0594 +**	**0.173 +**	0.031 -	**0.0769 +**
H4	-114010.84	0	**0.77 +**	**0.783 +**	**1 +**	**0.783 +**	**0.943 +**	**0.764 +**	**0.809 +**

Click here to access/download

Table

Table 1. Morphometric data based two pupulation_final2.docx

Table 2

Author statement

Wanying Liao: Conceptualization, Investigation, Validation, Visualization, Writing–Original Draft; Funding acquisition;
Pedro Henrique Campello-Nunes: Conceptualization, Investigation, Validation, Visualization, Writing–Original Draft; Funding acquisition;
Leandro Gammuto: Conceptualization, Investigation, Visualization, Validation, Writing–Original Draft, Software;
Tiago Abreu Viana: Conceptualization, Investigation, Visualization;
Roberto de Oliveira Marchesini: Investigation; Funding acquisition;
Thiago da Silva Paiva: Conceptualization, Writing–Review & Editing; Funding acquisition;
Inácio Domingos da Silva-Neto: Conceptualization, Investigation, Writing–Review & Editing, Supervision; Funding acquisition;
Letizia Modeo: Conceptualization, Investigation, Writing–Review & Editing, Supervision;
Giulio Petroni: Conceptualization, Investigation, Writing–Review & Editing, Supervision; Funding acquisition;